

Supporting Information for

**Discovery of a Cryptic Antifungal Compound from *Streptomyces albus*
J1074 Using High-Throughput Elicitor Screens**

Fei Xu¹, Behnam Nazari^{1, &}, Kyuho Moon^{1, &}, Leah B. Bushin^{1, &}
Mohammad R. Seyedsayamdost^{1, 2, *}

¹Department of Chemistry, Princeton University, Princeton, NJ 08544

²Department of Molecular Biology, Princeton University, Princeton, NJ 08544

[&]These authors contributed equally

*Correspondence should be addressed to M.R.S: mrseyed@princeton.edu

Table of contents		Pages
Methods		
Bacterial Strains and Plasmids		S3
DNA Manipulation and Construction of Mutants		S3
High-Throughput Elicitor Screen		S4
Reverse Transcription Quantitative PCR		S5
Small-scale Fermentation and Work-up of <i>S. albus</i> J1074		S6
Low-Resolution and High-Resolution HPLC-MS and HPLC Systems		S6
Large-scale Fermentation of <i>S. albus</i> J1074		S7
Purification and Structural Elucidation of Surugamides G-J		S7
Purification and Structural Elucidation of Albucyclones A-F		S7
Purification and Structural Elucidation of Acyl-surugamide A		S8
Purification and Structural Elucidation of Albuquinone A		S8
Purification and Structural Elucidation of Surugamides F2 and F3		S8
Antibiotic and Cathepsin B Inhibition Assays		S8
Supplementary Tables		
Table S1	Annotation of the surugamide biosynthetic gene cluster (<i>sur</i>)	S10
Table S2	Strains and plasmid used and generated in this study	S11
Table S3	Primers and qPCR parameters....	S12
Table S4	HR-MS data for surugamide G-J....	S13
Table S5	HR-MS/MS data for surugamide I....	S14
Table S6	NMR assignments of surugamide I....	S16
Table S7	NMR assignments of surugamide J, H, and G.....	S17
Table S8	NMR assignments of acyl-surugamide A....	S18
Table S9	NMR assignments of albucyclone A....	S19
Table S10	NMR assignments of albucyclone F in CD ₃ OD	S20
Table S11	NMR assignments of albucyclone D and E CD ₃ OD	S21
Table S12	NMR assignments of albuquinone A and....	S22
Supplementary Figures		
Figure S1	Genotype validation of three double crossover mutants....	S23
Figure S2	Analysis of RNA integrity used for qPCR experiments....	S24
Figure S3	Detection of the products of the <i>sur</i> cluster in wt <i>S. albus</i> J1074....	S25
Figure S4	UV-visible absorption spectra of....	S26
Figure S5	NMR spectra (800 MHz) of surugamide I....	S27
Figure S6	NMR spectra (800 MHz) of surugamide J....	S29
Figure S7	NMR spectra (800 MHz) of surugamide H....	S30
Figure S8	NMR spectra (500 MHz) of surugamide G....	S32
Figure S9	NMR spectra (800 MHz) of acyl-surugamide A....	S33
Figure S10	Additional evidence for the acyl group in acyl-surugamide A....	S35
Figure S11	NMR spectra (800 MHz) of albucyclone A....	S36
Figure S12	Additional evidence for attachment of the quinone moiety....	S38
Figure S13	NMR spectra (800 MHz) of albucyclone F....	S39
Figure S14	HR-MS/MS fragmentation analysis of albucyclone B.	S41
Figure S15	HR-MS/MS fragmentation analysis of albucyclone C.	S42
Figure S16	NMR spectra (800 MHz) and HR-MS/MS fragmentation of albucyclone D....	S43
Figure S17	HR-MS/MS fragmentation analysis of albucyclone E.	S45
Figure S18	NMR spectra (500 MHz) of albuquinone A....	S46
Figure S19	HR-MS/MS analysis of surugamide F2 compared with surugamide F.	S47
Figure S20	HR-MS/MS analysis of surugamide F3 compared with surugamide F.	S48
Figure S21	Biosynthetic model for surugamides in <i>S. albus</i>	S49
Figure S22	Induction of SOS response genes <i>recA</i> and <i>lexA</i> by etoposide.	S50
Supplementary References		S51

Methods

Bacterial Strains and Plasmids

The wild type strain of *Streptomyces albus* J1074 was kindly provided by the laboratory of Prof. Roberto Kolter at Harvard Medical School (Boston, MA). *eGFP* was kindly provided by the laboratory of Prof. Zemer Gitai at Princeton University (Princeton, NJ). *E. coli* strains ET12567 and BW25113, and plasmids pSET152, pIB139 and pJTU1289 were kindly provided by the laboratory of Prof. Zixin Deng at Shanghai Jiao Tong University (Shanghai, China). *XylE* was kindly provided by the laboratory of Prof. Mervyn Bibb at the John Innes Centre (Norwich, UK).

DNA Manipulation and Construction of Mutants

To generate the *S. albus attB::P_{ermE}-eGFP* reporter constructs, an *eGFP* fragment without a ribosomal binding site (RBS) was amplified by PCR using the corresponding primers (Table S2). The PCR fragment was digested with NdeI/EcoRI, along with plasmid pIB139, which contains the *ermE* promoter element¹. After ligation and amplification in *E. coli* DH5 α , pAttP::*P_{ermE}-eGFP* was obtained (Table S1). This plasmid was digested with EcoRI. A second copy of *eGFP* containing an RBS was PCR-amplified with appropriate primers (Table S2) and digested with MfeI/EcoRI. Ligation into pAttP::*P_{sur}-eGFP* afforded pAttP::*P_{ermE}-eGFPx2*. This process was repeated to give pAttP::*P_{ermE}-eGFPx3*. A similar strategy was used in making pAttP::*P_{ermE}-xylE* reporter integration plasmids. In this case, the *xylE* fragment was PCR-amplified from pIJ4083 using the primers shown (Table S2). The plasmids pAttP::*P_{ermE}-eGFP*, pAttP::*P_{ermE}-eGFPx2*, pAttP::*P_{ermE}-eGFPx3*, and pAttP::*P_{ermE}-xylE* were transformed into *E. coli* ET12567 by heat shock (see Table S1). Conjugation into *S. albus* was carried out as described below.

To generate *S. albus P_{sur}-eGFP* constructs, the *P_{sur}* promoter region (~260 bp) upstream of *surE* was selected using the BPROM website:

(<http://www.softberry.com/berry.phtml?topic=bprom&group=programs&subgroup=gfindb>).

This region (*P_{sur}*), along with *xylE* and *eGFP* were PCR-amplified and adjoined using overlap extension PCR to generate *P_{sur}-xylE* and *P_{sur}-eGFP*. These were cloned into plasmid pSET152, and subsequently, two additional copies of *eGFP* were added from MfeI/EcoRI-digested fragments, as described above, thus yielding plasmids pAttP::*P_{sur}-eGFPx3* and pAttP::*P_{sur}-xylE* (see Table S1 and Figure 1C). These two plasmids were transformed into *E. coli* ET12567 by heat shock and conjugation into *S. albus* carried out as described below.

To generate the *surE::eGFPx3* reporter construct, a ~2 kb region upstream of *surE* was amplified with the appropriate primers (Table S2). Then overlap extension PCR was carried out to fuse this fragment with *eGFP*. This construct was cloned into pJTU1278 using restriction enzymes BamHI and EcoRI. Subsequently, two additional *eGFP* copies, amplified and digested with MfeI/EcoRI, were added as described above. Finally, a ~2 kb region downstream of *surE* was amplified with appropriate primers (Table S2), digested with EcoRI/HindIII, and ligated into the vector containing the upstream region of *surE* adjoined to *eGFPx3*, to give p*SurE::eGFPx3* (see Table S1). This plasmid contains the proper construct consisting of 2 kb regions up- and down-stream of *surE*, with three copies of *eGFP* in the middle and was used for chromosomal replacement of *surE* with three copies of *eGFP*. The plasmid was transformed into *E. coli* ET12567 by heat shock and conjugation was carried out as described below.

To create the *surR* gene replacement plasmid (p Δ *surR*, see Table S1), ~2 kb regions up- and down-stream of *surR* were amplified using appropriate primers (Table S2) and digested with XbaI and HindIII. Each fragment was in turn cloned into pIJ2581 to create a contiguous 2 kb inserted fragment with a HindIII restriction site in the middle. The plasmid was amplified in *E. coli* DH5a and digested with HindIII. The apramycin resistance gene (*apr*) fused to *oriT* was amplified by PCR with appropriate primers from vector pIJ773. This was then digested with HindIII and ligated into the pIJ2581 vector containing the 2 kb insert, thus yielding the pIJ2581 construct containing a fragment

that comprises 2-kb-up-*surR_oriT-apr_2-kb-dn-surR*, which was used for generating the *surR::apr* gene inactivation mutant as described below. This plasmid ($p\Delta surR$) was transformed into *E. coli* ET12567 by heat shock and conjugation performed as outlined below.

For generating the *surA* and *surB* gene replacement plasmids ($p\Delta surA$ and $p\Delta surB$, see Table S1), the PCR-targeting gene replacement strategy was employed according to standard protocols². Briefly, a 4.8 kb internal fragment of *surA* was amplified by PCR, ligated into pJTU1289 (Tsr^R), and subsequently transformed into *E. coli* BW25113, which contains the λ Red plasmid pIJ790, to give pJTU1289-*surA_int*. A separate linear fragment was generated containing a fused *oriT-apr* (obtained from pIJ773) flanked by 40 bp regions that were homologous to internal regions of *surA* (about 700 bp apart). Electrocompetent *E. coli* BW25113 containing pJTU1289-*surA_int* and pIJ790 were cultured in LB in the presence of a final concentration of 10 mM L-arabinose to an OD_{600 nm} of 0.4-0.6 at 30°C and then electrotransformed with the linear fragment. Apramycin-resistant colonies were selected on LB-Agar containing 50 μ g/mL apramycin. The correct construct was verified by restriction endonuclease and DNA gel electrophoresis analysis. A similar strategy was used to generate the *surB* gene replacement plasmid. The plasmids ($p\Delta surA$ and $p\Delta surB$) were transformed into *E. coli* ET12567 by heat shock and conjugation performed as described below.

Conjugation of all the plasmids into *S. albus* used the following protocol: The plasmids (Apr^R) were all transformed into *E. coli* ET12567 (Cm^R) containing pUZ8002 (Kan^R), as described above. Conjugation was performed using the spores of *Streptomyces albus* J1074 (grown on SFM medium) according to standard methods³. Briefly, *E. coli* ET12567 containing the desired plasmids was cultured in LB containing Apr (50 μ g/mL), Kan (50 μ g/mL), and Cm (25 μ g/mL) to an OD_{600 nm} of ~0.4. The cells were collected by centrifugation and washed with LB to remove the antibiotics. *S. albus* spores were washed with TES buffer (50 mM, pH 8.0), collected, resuspended in 500 μ L TES buffer, and heat shocked at 50°C for 10 min. Spore stock was then supplemented with 500 μ L of 2x spore activating media, and then cultured at 37°C for 2h. The spore stocks and *E. coli* donor cells were collected and resuspended in equal amounts of LB media and subsequently mixed together. They were then plated on SFM agar plates (2% soybean meal in tap water, sterilized by autoclave, then filtered and mixed with 2% mannitol and 2% agar, and then autoclaved again) and grown for 16-20 h. The *attB*-integration mutant exconjugants were selected with 35 μ g/mL Apr and 50 μ g/mL Tmp (trimethoprim), while the double-crossover knockout mutant exconjugants were selected with 25 μ g/mL Tsr, 35 μ g/mL Apr, and 50 μ g/mL Tmp. For the *attB*-insertion, mutants were verified by PCR. For double-crossover mutants, exconjugants were first cultured in TSBY medium without any antibiotics. Surviving cells were subcultures again in TSBY medium. They were then diluted to obtain single colonies on SFM agar plates. The colonies were tested individually and separately for Apr-resistance and Tsr-susceptibility. The desired mutants were verified by PCR (see Fig. S1).

High-Throughput Elicitor Screen

Seed cultures for the reporter strains *sur::eGFPx3*, *attB::P_{sur}-eGFPx3*, negative control wild-type, and positive control *attB::P_{ermE}-eGFPx3* inoculated by transferring fresh spores ($\sim 10^7$) into 20 mL of YEME medium (per L: 3% (w/v) yeast extract, 5% peptone, 3% malt extract, 1% glucose and 10.7% sucrose, and 5mM MgCl₂•6H₂O) in a 125 mL Erlenmeyer flask equipped with stain-less steel springs. The cultures were grown at 30°C and 250 rpm for 3 days. Mycelia from each of the four cultures were collected by centrifugation (10 min, 3000g, RT) and diluted into 150 mL of R4 medium to give a final concentration of 0.05% (w/v). R4 medium consisted of (per L) 0.5% (w/v) glucose, 0.1% yeast extract, 0.5% MgCl₂•6H₂O, 0.2% CaCl₂•2H₂O, 0.15% proline, 0.118% valine, 0.28% TES, 50 mg/L casamino acid, 100 mg/L K₂SO₄, and 1x trace element solution, which contains 40 mg/L ZnCl₂, 200 mg/L FeCl₃•6H₂O, 10 mg/L CuCl₂•2H₂O, 10 mg/L MnCl₂•4H₂O, 10 mg/L Na₂B₄O₇•10H₂O, and 10 mg/L (NH₄)₆Mo₇O₂₄•4H₂O.⁴

Subsequently, the two reporter strains (*sur::eGFPx3* and *attB::P_{sur}-eGFPx3*) were each dispensed into 5 x sterile, clear-bottom 96-well plates (150 μ L per well) using a MultiFlo Microplate Dispenser (BioTek). A separate sterile 96-well separate plate was prepared for positive and negative controls; it

contained the negative control (wt *S. albus* J1074) in columns 1–3, *sur::eGFPx3* in columns 4–6, *attB::P_{sur}-eGFPx3* in columns 7–9, and the positive control *attB::P_{ermE}-eGFPx3* in columns 10–12 of the plate. No elicitors were added to the control plates. For strains *sur::eGFPx3* and *attB::P_{sur}-eGFPx3*, candidate elicitors were added from a commercially-available 502-member Natural Products Library (Enzo Scientific, catalog #BML-2865) using a CyBi-Well automated liquid transfer robot (CyBio). A volume of 0.4 μ L was transferred from the compound library into each well to give a final concentration of \sim 33 μ M. Upon additional of the compound library, t=0 fluorescence reads were recorded on a Synergy H1MF plate reader (BioTek) using λ_{ex} = 485 nm and λ_{em} = 505–650 nm in 5 nm steps. The plates were then sealed with an air-permeable membrane and the plates incubated at 30°C and 250 rpm for 60 h in Multitron Shaker (ATR) equipped with green sealing trays. To maintain constant humidity, several 1-L Erlenmeyer flasks containing 200 mL of water were also placed inside the shaker. After 60 h, end-point fluorescence was determined as described above. Fluorescence emission at 514 nm at 60 h was subtracted from that at t=0 and the data normalized to the fluorescence intensity of the positive control to give the plots depicted in Fig. 2.

Z' scores was calculated according to Eq. 1, where σ_p and σ_n correspond to the standard deviation in fluorescence emission for the positive (*attB::P_{ermE}-3XeGFP*) and negative (*sur::3XeGFP* or *attB::P_{sur}-3XeGFP* in the absence of elicitors) controls, respectively, and μ_p and μ_n correspond to the mean fluorescence emission for the positive and negative controls among the replicates⁵.

$$Z' = 1 - \{3 \times (\sigma_p + \sigma_n) / (\mu_p - \mu_n)\} \quad (\text{Eq. 1})$$

Reverse Transcription Quantitative PCR

All operations involving RNA utilized a dedicated RNase-free work area. To commence the experiment, seed cultures of wt *S. albus* J1074 were prepared by inoculating 3 mL of TSBY medium (3% (w/v) tryptic soy broth and 0.5% yeast extract) in a sterile 14 mL bacterial culture tube with freshly-prepared spores (\sim 10⁷)⁷. The culture was incubated at 30°C and 250 rpm in an Ecotron Shaker (ATR). After 48 hours cultivation, the cells were collected by centrifugation and subsequently diluted to a final concentration of 0.05% (w/v) in 250 mL Erlenmeyer flask containing 50 mL of R4 medium. Desired elicitors were added to final concentrations indicated in the figures (typically 1–100 μ M), and the cultures were incubated at 30°C and 250 rpm. After 48 h, 1 mL was removed from each sample and transferred to a 1.5 mL RNase-free Eppendorf tube (Ambion). Each sample was centrifuged (16,000g, 3 min) to collect the cells, the supernatant discarded, the cells flash-frozen in liquid N₂, and stored at -80°C.

RNA isolation was carried out using the Qiagen RNeasy kit following the manufacturer's instructions without modifications. Upon isolation, contaminating DNA was removed using the DNA-free kit (Ambion) according to manufacturer's instructions. Gel electrophoreses subsequently confirmed RNA integrity (Fig. S2). Finally, total RNA was converted into cDNA via the PrimeScript™ RT reagent Kit (Takara) using random hexamers as primers and 500 ng of each RNA sample as template.

Three genes (*surA*, *surC* and *surR*) were chosen for quantification by RT-qPCR. The primers were designed using primer-3-plus software available online. The primers were carefully chosen to give an amplicon length of 130–160 bp and a melting temperature of 60°C, though this was later optimized (see below & Table S2). The primers were chosen to vary in length between 18–22 bp, and, if possible, to contain a single G/C clamp at the 3' end. To ensure optimal qPCR parameters, the genomic DNA of *S. albus* J1074 was isolated using the Wizard genomic DNA purification kit (Promega), and each amplicon was subsequently amplified using standard PCR conditions with a high-fidelity, proof-reading Q5 DNA polymerase (NEB). The PCR reactions were then separated on a 1.2% agarose gel, the amplicon excised, and gel-extracted with the Gel Extraction kit (Qiagen). The extracted DNA was used to optimize qPCR conditions. Using the amplicon template, the primer concentrations were first varied followed by the annealing/extension temperatures, which ranged from 58–68°C in eight steps. The combination that gave the lowest quantification cycle (Cq) was

used in the experiments (Table S2). The C_q was obtained with an automatic baseline determined by the CFX Manager Software (Bio-Rad). As positive controls, these standards were included in every plate that contained the experimental samples, along with no-DNA controls, in duplicates.

qPCR analysis was performed on a CFX96 Real-Time PCR Detection System (Bio-Rad) consisting of a C1000 Thermal Cycler and a CFX96 Real-Time System. The reaction was carried out in hard-shell, clear 96-well qPCR plates (Bio-Rad) and utilized the iTaq Universal SYBR Green Supermix (Bio-Rad). Each well, in a total volume of 16 μ L, contained 8 μ L of iTaq Supermix, 1 μ L of standard DNA or cDNA, 1 μ L of each primer and 5 μ L of DEPC-treated water (Invitrogen). The PCR cycle consisted of 1-min incubation at 95°C followed by 42 cycles of a 2-step amplification protocol (5 s at 95°C, then 30 s at annealing/extension temperature). This was followed by a denaturation cycle to determine the melting temperature of the amplicon, where a single species was observed in all experiments reported.

Relative quantification was used to determine the levels of each transcript as a function of elicitor. The C_q for each sample was determined in triplicates. The resulting value was then normalized using internal standard GAPDH and further normalized to the DMSO control sample to give the fold-change for that amplicon as a function of elicitors shown in Fig. 2C. The concentrations of elicitors used are indicated in the figure legend.

Small-scale Fermentation and Work-up of *S. albus* J1074

For comparative small-scale fermentations, mutant and wt strains were grown side-by-side in the same media and worked up in identical fashion. Seed cultures of wt *S. albus* J1074 were prepared by inoculating 3 mL of TSBY medium in a sterile 14 mL bacterial culture tube with freshly-prepared spores ($\sim 10^7$). The culture was incubated at 30°C and 250 rpm for 2-3 days, then diluted into 50 mL of R4 medium (in a 250 mL Erlenmeyer flask) to a final concentration of 0.05% (w/v). Elicitors were added to the R4 medium at the start of growth at desired concentrations (indicated in figure legends). The cultures were grown at 30°C and 200 rpm. After ~ 4 days, cells were removed by centrifugation and the resulting supernatant was extracted twice with 30 mL of ethyl acetate. The organic phases were combined, dried in vacuo, dissolved in 100 μ L MeOH and analyzed by low-resolution HPLC-ESI-MS and/or high-resolution (HR) HPLC-Qtof-MS.

Low-Resolution and High-Resolution HPLC-MS and HPLC Systems

Low-Resolution and High-Resolution HPLC-MS

Low resolution (LR) HPLC-MS analysis was performed on an Agilent 1260 Infinity Series HPLC system equipped with an automated liquid sampler, a diode array detector, and a 6120 Series ESI mass spectrometer using a reversed phase Luna C18 column (Phenomenex, 5 μ m, 150 \times 4.6 mm). The mobile phase consisted of water and MeCN (both contained 0.1% formic acid). Upon injection, elution was carried out isocratically with 10% MeCN (3 min) followed by a linear gradient from 10%–90% MeCN over 20 min, and 90–100% MeCN over 5 min, at a flow rate of 0.6 mL/min. HR HPLC-MS and HR-tandem HPLC-MS were carried out on an Agilent 6540 UHD Accurate Mass Q-tof LC-MS system, which consists of a 1260 Infinity Series HPLC system, an automated liquid sampler, a diode array detector, a JetStream ESI source, and the 6540 Series Q-tof. The MS was calibrated to <1 ppm. Samples were resolved on the same Luna C18 column under the same gradient program as described above with a flow rate of 0.4 mL/min.

HPLC Purification Systems

HPLC purifications were carried out on an Agilent preparative HPLC system containing a 1260 Infinity series binary pump, a diode array detector, and an automated fraction collector. Semi-preparative or analytical-scale purifications were performed on an Agilent HPLC system containing a 1260 Infinity Series binary pump or a 1290 Infinity quaternary pump. Each system was equipped with an automatic liquid sampler, a temperature-controlled column compartment, a diode array detector, and an automated fraction collector. Unless indicated otherwise, the mobile phase used consisted of water+0.1% formic acid and MeCN+0.1% formic acid.

Large-scale Fermentation of *S. albus* J1074

Large-scale fermentation was carried out as described above. *S. albus* J1074 seed cultures were prepared by inoculating 50 mL of TSBY medium in a 250 mL Erlenmeyer equipped with stainless steel springs with spore stocks. The culture was grown for 2-3 days at 30°C and 250 rpm, then diluted to a final concentration of 0.05% (w/v) in 10-20 x 2 L Erlenmeyer flasks each containing 200 mL R4 medium, supplemented with ivermectin (final concentration of 30 µM). The production cultures were grown at 30°C and 250 rpm for 7 days. Then, the cells were harvested by centrifugation and the cell pellets extracted twice with ~100 mL of 1:1 MeOH/Acetone. The extracts were combined, dried in vacuo, and stored in the refrigerator until further purification. Meanwhile, the separated supernatant was extracted twice with an equal volume of ethyl acetate and the resulting organic phase dried over Na₂SO₄ and subsequently evaporated to dryness in vacuo.

Next HPLC-MS was carried on both the cell pellet and supernatant extracts. About 0.1 mg of dried material was resuspended in 50 µL MeOH, the suspension filtered, ~5 µL injected onto the HPLC-Qtof-MS, and subsequently eluted as described above. The analysis showed that surugamide G-J and pyrisurugamide A and B were present in both cell pellet and supernatant extracts. Acyl-surugamide A, albucyclones A-F, albuquinone A, and surugamide F2 and F3 were only found in the cell pellet extracts. The purifications of these different groups of compounds are described below.

Purification and Structural Elucidation of Surugamides G-J

Surugamides G-J were purified from 4 L fermentation of *S. albus* in the presence of ivermectin as described above. After fermentation, the cell pellets were harvested by centrifugation yielding ~300 g of cell paste, which was extracted twice with 2 L of 1:1 MeOH/acetone. The combined extract was evaporated to dryness in vacuo, resuspended in 40 mL MeOH, and subsequently purified on an Agilent 1260 Infinity Series Preparative HPLC equipped with a diode array detector and an automated fraction collector. The material was resolved on a preparative Luna C18 column (Phenomenex, 5 µm, 21.2 x 250 mm) operating at 12 mL/min with mobile phases consisting of water and MeCN (+0.1% formic acid). Upon injection, elution was carried out isocratically with 20% MeCN for 4 min, followed by a linear gradient of 20-100% MeCN over 20 min. Fractions were collected in 1 min intervals over the time range of 6-28 min. All fractions were subjected to LR-HPLC-MS analysis as described above using a 40 µL injection volume. Fractions that contained surugamides G-J were pooled, dried in vacuo, resuspended in a small volume of MeOH and further purified on a semi-preparative/analytical Agilent HPLC purified system. The sample loaded onto a semi-preparative RP Amide-C16 column (Supelco, 5 µm, 10 x 250 mm) operating at 2.5 mL/min with the mobile phase as above and gradients of 15-50% MeCN over 50 min followed by 50-100% MeCN over 10 min. The fractions were analyzed again by LR-HPLC-MS. Samples containing pure surugamide G-J were combined, and lyophilized to dryness. This procedure gave pure surugamides G (1.5 mg), H (1.8 mg), I (7 mg), and J (0.7 mg).

The HR-ESI-MS data obtained for these surugamides and the molecular formula are listed in Table S4. To solve their structures, comprehensive NMR data sets were acquired at the Princeton University Department of Chemistry NMR Facilities. All 1D/2D NMR spectra were collected in MeOH-*d*₄ in the triple resonance cryoprobe of an A8 Avance III HD 800 MHz NMR spectrometer (Bruker). NMR data were analyzed in MestReNova (MestreLab Research).

Purification and Structural Elucidation of Albucyclones A-F

To purify albucyclones A-F, 8 L of *S. albus* J1074 were cultured in the presence of ivermectin as described above for surugamides and pyrisurugamides. After fermentation, the cell pellets were removed by centrifugation (RT, 8000g, 30 min) on a Beckman-Coulter Avanti J26-XP centrifuge, and the supernatant extracted twice with an equal volume of ethyl acetate. The organic layers were combined, treated with Na₂SO₄, and then evaporated to dryness in vacuo. The residue was dissolved in 35 mL MeOH and purified by HPLC using a preparative Luna C18 column (Phenomenex, 5 µm, 21.2 x 250 mm) operating at 12 mL/min with the same elution program as used for surugamides: 20% MeCN for 4 min, followed by a gradient from 20-100% MeCN over 20 min.

Fractions were collected in 1 min intervals from 4-30 min and monitored by HR-HPLC-MS for presence of albucyclones (40 μ L injection). Those containing acyl-surugamide A, albuquinone, and surugamide F were collected, dried and stored at 4°C until further purification. Fractions containing albucyclones were pooled, dried and further resolved on a semi-preparative RP Amide-C16 column (Supelco, 5 μ m, 10 x 250 mm) operating at 2.5 mL/min. Upon injection, samples were eluted isocratically (40% MeCN for 30 min) followed by 40-100% linear gradient over 8 min. with same linear gradient step: 40% B to 58% B (0-30 min), 100% B (30-38 min) (A, Milli-Q H₂O; B, MeCN). For final purifications, fractions containing albucyclones were injected on an analytical Luna C18 column (Phenomenex, 5 μ m, 4.6 x 250 mm) and eluted as described above for the semi-preparative column, but using a flow-rate of 1 mL/min. This procedure yielded pure albucyclone A (1.8 mg), B (0.4 mg), C (0.5 mg), D (0.6 mg), E (0.5 mg) and F (1.5 mg). They were characterized by HR-MS, HR-MS/MS and 1D/2D NMR.

Purification and Structural Elucidation of Acyl-surugamide A

Dried fractions containing acyl-surugamide A (from the preparative Luna C18 column, see last paragraph) were dissolved in MeOH and purified further on semi-preparative Luna C18 column (Phenomenex, 5 μ m, 10 x 250 mm) with a flow-rate of 2.5 mL/min. Elution was carried out with 30% MeCN over 5 min, followed by linear gradients consisting of 30-40% over 26 min and 40-100% over 8 min. Fractions containing acyl-surugamide A, as detected by HR-HPLC-MS, were pooled and dried yielding 0.6 mg of pure material. Subsequently, HR-MS and 1D/2D NMR was carried out for structural elucidation.

Purification and Structure Elucidation of Albuquinone A

Dried fractions containing albuquinone A (from preparative Luna C18 column, see "Purification and structural elucidation of albucyclones A-F") were dissolved in MeOH and purified further on a semi-preparative RP Amide-C16 column (Supelco, 5 μ m, 10 x 250 mm). Elution was carried out with a flow-rate of 2.5 mL/min and linear gradients consisting of 12-19% MeCN over 27 min, and 19-100% MeCN over 7 min. This procedure yielded 0.3 mg pure albuquinone A, which was subsequently characterized by HR-MS and 1D/2D NMR.

Purification and Structural Elucidation of Surugamides F2 and F3

Dried fractions containing surugamide F analogs (from preparative Luna C18 column, see "Purification and structural elucidation of albucyclones A-F") were dissolved in MeOH and purified further on a semi-preparative RP Amide-C16 column (Supelco, 5 μ m, 10 x 250 mm) operating at 2.5 mL/min. Elution was performed with a linear gradient of 30-40% MeCN over 30 min and 40-100% MeCN over 8 min. Samples containing surugamide F variants, as determined by HR-MS/MS, were resolved further on an analytical Luna C18 column (Phenomenex, 5 μ m, 4.6 x 250 mm). Elution was carried out with a flow-rate of 1 mL/min and a linear gradient of 40-44% MeCN over 30 min, followed by 44-100% MeCN over 8 min. This procedure gave pure surugamide F (0.5 mg), surugamide F2 (<0.2 mg) and surugamide F3 (<0.2 mg). The structures of surugamide F2 and F3 were elucidated using targeted HR-tandem-MS with varying collision energies (25, 35, 45, 55 V) on the Agilent HPLC-Qtof-MS instrument described above. Fragment ions from the various runs were combined and analyzed in MassHunter software. These unambiguously revealed the linear sequence of surugamide F2. In the case of surugamide F3, we could not distinguish between Ile and Leu at position 7 of the linear peptide (see Fig. 4F).

Antibiotic and Cathepsin B Inhibition Assays

Bacillus subtilis 168, *E. coli* K12, *Pseudomonas aeruginosa* PAO1, *Enterococcus faecalis* OG1RF, *Staphylococcus aureus* Newman, *Saccharomyces cerevisiae* and *Saccharomyces pombe* were used for antibiotic assays. *B. subtilis* (30°C), *E. coli* (37°C), *P. aeruginosa* (30°C), and *E. faecalis* (37°C) were cultured in LB medium at the temperatures indicated. *S. aureus* was cultured in Brain-Heart-Infusion (BHI) medium at 37°C. *S. cerevisiae* and *S. pombe* were grown at 25°C in YPM medium (0.5% yeast extract, 0.3% peptone, 2.5% mannitol), and YES medium (0.5% yeast extract, 3% glucose, 225 mg/L leucine, 225 mg/L histidine, 225 mg/L adenine, 225 mg/L uracil), respectively. The

assays were carried out in accordance with the 2003 guidelines of the Clinical and Laboratory Standards Institute (CLSI) using the microtiter method. Briefly, microbial seed cultures were initiated by inoculating 3 mL of the indicated medium each strain and by growing these overnight at the indicated temperatures. Each culture was then diluted to an initial OD_{600 nm} of 0.02 in 100 µL volume per well in a 96-well plate, which gave an inoculum of $\sim 5 \times 10^5$ to 5×10^6 cells. The wells contained varying concentrations of the compounds tested: 0, 0.02, 0.04, 0.1, 0.2, 0.4, 1, 2, 4, 10, 20, 40, 100 µM final concentration. Assays were set-up in triplicates. The plates were then incubated at the temperatures listed above without shaking and OD_{600 nm} determined after 16 h (bacteria) or 40 h (yeast). The compounds used for antibiotic assays included surugamide, pyrisurugamide A, albuquinone, acyl-surugamide A, albucyclones.

Cathepsin B inhibition assays were carried as previously reported using the Cathepsin B Inhibition assay kit (Sigma-Aldrich).^{8,9} The fluorescence-based assays was conducted in a final volume of 50 µL according to manufacturer instructions. Fluorescence emission was determined in a microtiter plate in kinetic mode (1 read per minute for 1 h) using a BioTek H1MF plate reader and $\lambda_{\text{ex}} \sim 400$ / $\lambda_{\text{em}} \sim 505$ nm. IC₅₀ values were subsequently calculated according to instructions.

Table S1. Annotation of the surugamide biosynthetic gene cluster (*sur*).

Orf name	Gene locus ID	Length (AA)	Homology-Based Predicted Function
orf1	XNR3458	475	Sulfoacetaldehyde dehydrogenase
orf2	XNR3457	269	Pimeloyl-ACP methyl ester carboxyesterase
orf3	XNR3456	85	MbtH protein
orf4	XNR3455	265	ABC transport system, membrane protein
orf5	Xnr3454	313	ABC transporter, ATP-binding protein
orf6	XNR3453	123	Hypothetical protein
SurR	XNR3452	138	GntR family DNA-binding transcriptional regulator
orf7	XNR3451	365	Putative membrane protein
SurE	XNR3450	451	Beta-lactamase
SurA	XNR3449	5733	NRPS (A-C-A-E-C-A-C-A-E-C-A)
SurB	XNR3448	4265	NRPS (A-C-A-E-C-A-C-A)
SurC	XNR3447	7691	NRPS (C-A-C-A-E-C-A-C-A-E-C-A-C-A-E)
SurD	XNR3446	4114	NRPS (C-A-C-A-E-C-A-E)
orf8	XNR3445	448	Drug resistance transporter, EmrB/QacA subfamily
orf9	XNR3444	203	TetR family transcriptional regulator
orf10	XNR3443	102	Hypothetical protein
orf11	XNR3442	524	EmrB/QacA subfamily drug resistance transporter
orf12	XNR3441	406	Secreted protein
orf13	XNR3440	329	Osmoprotectant transport system, substrate-binding protein
orf14	XNR3439	253	Osmoprotectant transport system, permease protein
orf15	XNR3438	236	Osmoprotectant transport system, permease protein

Table S2. Strains and plasmids used and generated in this study.

Strain/Plasmid	Purpose	Source
Strains		
<i>E. coli</i> DH5 α	Host strain for cloning	NEB
<i>E. coli</i> BW25113	Host strain for PCR targeting method	Deng Lab
<i>E. coli</i> ET12567	Donor strain for conjugation	Deng Lab
<i>E. coli</i> K12	Test strain for bioactivity assay	Kolter Lab
<i>Bacillus subtilis</i> 168	Test strain for bioactivity assay	ATCC
<i>Pseudomonas aeruginosa</i> PAO1	Test strain for bioactivity assay	ATCC
<i>Staphylococcus aureus</i> Newman	Test strain for bioactivity assay	ATCC
<i>Enterococcus faecalis</i> OG1RF	Test strain for bioactivity assay	Kolter Lab
<i>Saccharomyces cerevisiae</i>	Test strain for bioactivity assay	Kolter Lab
<i>Saccharomyces pombe</i>	Test strain for bioactivity assay	Zakian Lab
<i>Streptomyces albus</i> J1074	Wild type strain	Kolter Lab
<i>surA::apr</i> (Δ <i>surA</i>)	<i>surA</i> inactivation mutant of <i>S. albus</i> J1074	This study
<i>surB::apr</i> (Δ <i>surB</i>)	<i>surB</i> inactivation mutant of <i>S. albus</i> J1074	This study
<i>surR::apr</i> (Δ <i>surR</i>)	<i>surR</i> inactivation mutant of <i>S. albus</i> J1074	This study
<i>surE::eGFPx3</i>	<i>eGFP</i> reporter for <i>sur</i> cluster	This study
<i>attB::P_{sur}-eGFPx3</i>	Neutral site <i>eGFP</i> reporter of <i>sur</i> cluster	This study
<i>attB::P_{sur}-XylE</i>	Neutral site <i>xylE</i> reporter of <i>sur</i> cluster	This study
<i>attB::P_{ermE}-XylE</i>	Positive control: <i>P_{ermE}</i> -controlled <i>xylE</i> reporter	This study
<i>attB::P_{ermE}-eGFP</i>	Positive control: <i>P_{ermE}</i> -controlled <i>eGFP</i> reporter	This study
<i>attB::P_{ermE}-eGFPx2</i>	Positive control: <i>P_{ermE}</i> -controlled <i>eGFPx2</i> reporter	This study
<i>attB::P_{ermE}-eGFPx3</i>	Positive control: <i>P_{ermE}</i> -controlled <i>eGFPx3</i> reporter	This study
Plasmid		
pSET152	Apr ^R , Vector for neutral site insertion	Deng Lab
pIB139	Apr ^R , Vector for neutral site insertion with <i>P_{ermE}</i>	Deng Lab
pSK ⁺	Amp ^R , cloning vector cloning	Deng Lab
pJTU1278	Amp ^R , Tsr ^R , conjugation vector	Deng Lab
pJTU1289	Amp ^R , Tsr ^R , conjugation vector	Deng Lab
pIJ773	Apr ^R , Vector for PCR targeting method	Deng Lab
p Δ <i>surA</i>	Amp ^R , Tsr ^R , Apr ^R , plasmid used for <i>surA</i> inactivation	This study
p Δ <i>surB</i>	Amp ^R , Tsr ^R , Apr ^R , plasmid used for <i>surB</i> inactivation	This study
p Δ <i>surR</i>	Amp ^R , Tsr ^R , Apr ^R , plasmid used for <i>surR</i> inactivation	This study
pAttP:: <i>P_{sur}-xylE</i>	Apr ^R , plasmid for neutral site insertion of <i>P_{sur}-XylE</i>	This study
pAttP:: <i>P_{sur}-eGFPx3</i>	Apr ^R , plasmid for neutral site insertion of <i>P_{sur}-eGFPx3</i>	This study
pAttP:: <i>P_{ermE}-xylE</i>	Apr ^R , plasmid for neutral site insertion of <i>P_{ermE}-xylE</i>	This study
pAttP:: <i>P_{ermE}-eGFP</i>	Apr ^R , plasmid used neutral site insertion of <i>P_{ermE}-eGFP</i>	This study
pAttP:: <i>P_{ermE}-eGFPx2</i>	Apr ^R , plasmid used neutral site insertion of <i>P_{ermE}-eGFPx2</i>	This study
pAttP:: <i>P_{ermE}-eGFPx3</i>	Apr ^R , plasmid used neutral site insertion of <i>P_{ermE}-eGFPx3</i>	This study
p <i>SurE</i> :: <i>eGFPx3</i>	Apr ^R , plasmid used replacement of <i>surE</i> with <i>eGFPx3</i>	This study

Table S3. Primers and qPCR parameters used for creating mutants and performing RT-qPCR.

Primer sequences		Primer functions	
5'-AAGCTTAGACGACCACCTTCGCGCTGTC-3' 5'-AAGCTTTAGACGGACGGGACGGCGTGCAGC-3'		Cloning <i>surA</i> fragments for making <i>surA::apr</i> mutant	
5'-AAGCTT ACGAGACCTGCGGACCGTCTCC-3' 5'-AAGCTTTCGTGCACCACCTGCACCGGCTGC-3'		Cloning <i>surB</i> fragments for making <i>surB::apr</i> mutant	
5'-TTCTTCGTCAACACCCTGGTCTGCGGCAGCAGGTGCCGGATTCCGGGGATCCGTCGACC-3' 5'-GACCGGGTGGTCCGGTGAAGGCTGAGGATGTCGTGGGCGATCTGTAGGCTGGAGCTGCTTC-3'		Cloning <i>Apr^R</i> gene cassette for <i>surA::apr</i>	
5'-AGATCAGCCACACCCTGATCCCGCCGACGGTCCCTCGCCAGATTCCGGGGATCCGTCGACC-3' 5'-CGAGGCTGAAGAAGTTGTCCCGGGTGCAGACAGTTCCACCTGTAGGCTGGAGCTGCTTC-3'		Cloning <i>Apr^R</i> gene cassette for <i>surB::apr</i>	
5'-ACTCTAGACTGAAGTTCTCCGGGCCACGAC-3' 5'-GTCGTACGGTCACCATCCTCTAGTCAAGCTTGCACAGCTTCAATCTATCTG-3'		Cloning the left arm of <i>surR::apr</i> knock out plasmid	
5'-CAAGCTTGACTAGAGGATGGTACCCTACGAC-3' 5'-GCTCTAGATGCCTCGCCTGCCTACCAGACTC-3'		Cloning the right arm of <i>surR::apr</i> knock out plasmid	
5'-AGTAAGCTTCCACCAGACTATTTGCAACAGT-3' 5'-ACCAAGCTTCGGGGTCAATATAGCGATTTT-3'		Generating the fused <i>surR::apr</i> fragment	
5'-ATCATCACGCCGCGAGCTGAGC-3' 5'-CGAGGACGAGGAGTTTCG-3'		Primers for validation of the genotype of <i>surA::apr</i> mutant	
5'-AGATCAGCCACACCCTGATCC-3' 5'-TGAAGAAGTTGTCCCGGGTGC-3'		Primers for validation of the genotype of <i>surB::apr</i>	
5'-GGATCC ATCAGTGCCATGGGGAGCTTCC-3' 5'-TTGCTCACCATTGGTCCCTGCGCCCACTGC-3'		Cloning left arm of <i>surE::eGFPx3</i> knockout plasmid	
5'-GAATTC ATGTTCCAGGATGACGCGTCCG-3' 5'-AAGCTT TCCAGGAACCAGAGCCGTTCTGC-3'		Cloning right arm of <i>surE::eGFPx3</i> knockout plasmid	
5'-AGGGGACGCAATGGTGAGCAAGGGCGAGG-3' 5'-GAATTC TCACTTGACAGCTCGTCCATG-3'		Generating the fused <i>surE::eGFPx3</i> fragment	
5'-TTTCCGCTGCTGCTGAAGCTG-3' 5'-TCGAGTTCGCGGTAGGTCAGG-3'		Primers for validation of the genotype of <i>surE::eGFPx3</i>	
5'-TTGCTCACCATTGGTCCCTGCGCCAC-3' 5'-AGGGGACGCAATGGTGAGCAAGGGCGAGG-3'		Cloning <i>Psur-eGFPx3</i> for pSET152 to generate <i>attB::Psur-eGFPx3</i>	
5'-ATCATATGATGGTGAGCAAGGGCGAGGAG-3' 5'-AAGAATTCTCACTTGTACAGCTCGTCCATG-3'		Cloning <i>eGFP</i> into <i>pIB139</i>	
5'-ACAATTGCAGCTCAAGGAGGATCCATCATGGTGAGCAAGGGCGAGGAG-3' 5'-AAGAATTCTCACTTGTACAGCTCGTCCATG-3'		Amplifying <i>eGFP</i> with RBS site	
5'-ATAAGCTTATGAACAAGGTGTAATGCG-3' 5'-AATCTAGATCAGGTCAGCACGGTCATG-3'		Cloning <i>xylE</i> for creating the <i>Psur-xylE</i> fragment for pSET152	
5'-GCTTCTAGAGGGCGCGCTGCTCAACGTGA-3' 5'-ACAAGCTTGCCTCCCTCCGCCAGTCAAC-3'		Cloning <i>Psur</i> for creating the <i>Psur-xylE</i> fragment for pSET152	
5'-ATCATATGATGAAAAAGGAGTTATGCG-3' 5'-AAGAATTCTCAGGTCAGCACGGTCATG-3'		Cloning <i>xylE</i> downstream of <i>P_{ermE}</i> to make <i>P_{ermE-xylE}</i>	
RT-qPCR primer sequences	Gene	A/E Temp (°C) ^a	Amplicon length (bp)
5'-CAAGACCGTCAAGGTGCTCT-3' 5'-GAGCCGAGATGATGACCTTC-3'	XNR4919 (<i>gapdh</i>)	64.4	158
5'-GAGAACTACCCGGACAACGA-3' 5'-GGGTCGTAGGAGAGGTCCAG-3'	XNR3449 (<i>surA</i>)	64.4	146
5'-GACGAGACCCTGTCTTACGC-3' 5'-AGTACGGTACGCACTCGAC-3'	XNR3447 (<i>surC</i>)	64.4	134
5'-AGGTCCCGATCTACCAGCA-3' 5'-GTAGGCCCTTGTGACGGTGT-3'	XNR3452 (<i>surR</i>)	64.4	143

^a Annealing-extension temperature used in the amplification cycle.

Table S4. HR-MS data for surugamide G–J, acyl-surugamide A, albuquinone A, albucyclones A–F, and surugamide F2–3.

Surugamide	$[M+H]^+_{\text{calc}}$	$[M+H]^+_{\text{obs}}$	Δppm
G	884.59734	884.59461	3.1
H	870.58169	870.57858	3.6
I	856.56604	856.56293	3.6
J	842.55039	842.54812	2.7
Acyl-surugamide	$[M+H]^+_{\text{calc}}$	$[M+H]^+_{\text{obs}}$	Δppm
A	982.67050	982.66930	1.2
Albucyclone	$[M+H]^+_{\text{calc}}$	$[M+H]^+_{\text{obs}}$	Δppm
A	1126.66648	1126.66302	3.1
B	1112.65083	1112.65108	0.2
C	1112.65083	1112.65154	0.6
D	1084.61953	1084.61643	2.9
E	1084.61953	1084.61596	3.3
F	1070.60388	1070.60141	2.3
Surugamide F	$[M+H]^+_{\text{calc}}$	$[M+H]^+_{\text{obs}}$	Δppm
F2	1042.63099	1042.62692	3.9
F3	1070.66139	1070.65397	6.9
Albuquinone	$[M+H]^+_{\text{calc}}$	$[M+H]^+_{\text{obs}}$	Δppm
A	219.07697	219.07242	20.8

Table S5. HR-MS/MS data for surugamide I, acyl-surugamide A, albucyclone B, surugamide F, surugamide F2, and surugamide F3.

Comounds/Sequence	Ion	[M+H] ⁺ _{calc}	[M+H] ⁺ _{expt}	Δppm
Surugamide I				
Val-Ala	y2	171.11335	171.11419	4.9
Val-Ala-Leu	y3	284.19742	284.19494	8.7
Val-Ala-Leu-Phe	y4	431.26583	431.26811	5.3
Val-Ala-Leu-Phe-Val	y5	530.33424	530.33712	5.4
Val-Ala-Leu-Phe-Val-Lys	y6	658.42921	658.43413	7.5
Val-Ala-Leu-Phe-Val-Lys-Val	y7	757.49762	757.50178	5.5
Val-Ala-Leu-Phe-Val-Lys-Val-Val	y8	856.56604	856.57062	5.3
acyl-surugamide A				
Ala-Ile	y2	185.12900	185.12921	1.1
Ala-Ile-Leu	y3	298.21307	298.21370	2.1
Ala-Ile-Leu-Phe	y4	445.28148	445.28215	1.5
Ala-Ile-Leu-Phe-Ile	y5	558.36544	558.36474	1.3
Ala-Ile-Leu-Phe-Ile-Lys*	y6	756.50237	756.50605	4.9
albucyclones B				
Lys*	y1	343.14051	343.14133	2.4
Lys*-Ile	y2	456.22469	456.22400	1.5
Lys*-Ile-Val	y3	555.29311	555.29254	1.0
Lys*-Ile-Val-Ala	y4	626.33022	626.32998	0.4
Lys*-Ile-Val-Ala-Ile	y5	739.41429	739.41307	1.6
Lys*-Ile-Val-Ala-Ile-Leu	y6	852.49835	852.49519	3.7
Lys*-Ile-Val-Ala-Ile-Leu-Phe	y7	999.56740	999.56676	0.6
Lys*-Ile-Val-Ala-Ile-Leu-Phe-Ile	y8	1112.65083	1112.65151	0.6
surugamide F				
Trp-Leu-Val-Thr	b4	500.28679	500.28956	5.5
Trp-Leu-Val-Thr-AMPA	b5	585.33955	585.33932	0.4
Trp-Leu-Val-Thr-AMPA-Leu	b6	698.42362	698.42337	0.4
Trp-Leu-Val-Thr-AMPA-Leu-Val	b7	797.49203	797.49116	1.1
Trp-Leu-Val-Thr-AMPA-Leu-Val-Ala	b8	868.52914	868.52993	0.9
Trp-Leu-Val-Thr-AMPA-Leu-Val-Ala-Val	b9	967.59756	967.59687	0.7
Val-Thr-AMPA-Leu-Val-Ala-Val-Ala	y8	757.48186	757.48056	1.7
Thr-AMPA-Leu-Val-Ala-Val-Ala	y7	658.41345	658.41355	0.2
AMPA-Leu-Val-Ala-Val-Ala	y6	557.36577	557.36617	0.7
Leu-Val-Ala-Val-Ala	y5	472.31300	472.31246	1.1

Val-Ala-Val-Ala	y4	359.22894	359.22964	1.9
surugamide F2				
Trp-Val-Val-Thr-AMPA-Leu	b6	684.40797	684.40538	3.8
Trp-Val-Val-Thr-AMPA-Leu-Val	b7	783.47638	783.47429	2.7
Trp-Val-Val-Thr-AMPA-Leu-Val-Ala	b8	854.51349	854.51717	4.3
Trp-Val-Val-Thr-AMPA-Leu-Val-Ala-Val	b9	953.58191	953.57877	3.3
Val-Val-Thr-AMPA-Leu-Val-Ala-Val-Ala	y9	856.55053	856.56446	16.3
Val-Thr-AMPA-Leu-Val-Ala-Val-Ala	y8	757.48212	757.47238	12.9
AMPA-Leu-Val-Ala-Val-Ala	y6	557.36577	557.36294	5.1
surugamide F3				
Trp-Leu-Val	b3	399.2396	399.23694	7.4
Trp-Leu-Val-Thr-AMPA-Leu	b6	698.42362	698.42374	0.2
Trp-Leu-Val-Thr-AMPA-Leu-Leu/Ile	b7	811.50819	811.50128	8.5
Trp-Leu-Val-Thr-AMPA-Leu-Leu/Ile-Ala-Val	b9	981.61371	981.61353	0.2
Thr-AMPA-Leu-Leu/Ile-Ala-Val-Ala	y7	672.42960	672.42184	11.5
AMPA-Leu-Leu/Ile-Ala-Val-Ala	y6	571.38192	571.38287	1.7

Table S6. NMR assignments for surugamide I in CD₃OD. The numbering scheme for surugamide I is shown below the table.

	Position	δ_c^a	δ_H^b (Multiplicity, Hz)	Position	δ_c^a	δ_H^b (Multiplicity, Hz)	
Val1	1	172.5		Val4	1	174.5	
	2	60.3	4.14 (d, 6.0)		2	62.4	3.64 (d, 8.0)
	3	30.9	2.19 (m)		3	30.4	1.72 (m)
	4	19.6	0.91 (d, 7.0)		4	19.9	0.80 (d, 7.0)
	5	18.3	0.88 (d, 7.0)		5	19.1	0.44 (d, 7.0)
Ala	1	175.1		Phe	1	174.0	
	2	50.3	4.22 (q, 7.0)		2	54.6	4.59 (m)
	3	18.8	1.35 (d7.0)		3	37.6	3.41 (m), 2.69 (m)
4	19.8	0.92 (m)	4		139.9		
Val2	1	175.1		5, 9	129.6	7.23 (m)	
	2	61.7	3.95 (m)	6, 8	130.1	7.23 (m)	
	3	30.2	2.02 (m)	7	127.9	7.16 (m)	
	4	19.8	0.92 (m)	Leu	1	175.9	
	5	19.5	0.98 (m)		2	54.7	4.33 (m)
Val3	1	173.6		3	41.1	2.09 (m), 1.58 (m)	
	2	62.1	3.96 (m)	4	26.2	1.76 (m)	
	3	31.1	2.10 (m)	5	23.9	0.98 (m)	
	4	19.9	0.97 (m)	6	21.6	0.92 (m)	
	5	18.5	0.95 (m)				
Lys	1	174.7					
	2	53.1	4.44 (br s)				
	3	32.4	1.69 (m), 1.59 (m)				
	4	23.4	1.25 (m)				
	5	27.5	1.55 (m), 1.46 (m)				
	6	40.7	2.88 (m), 2.83 (m)				

^a200 MHz, ^b800 MHz

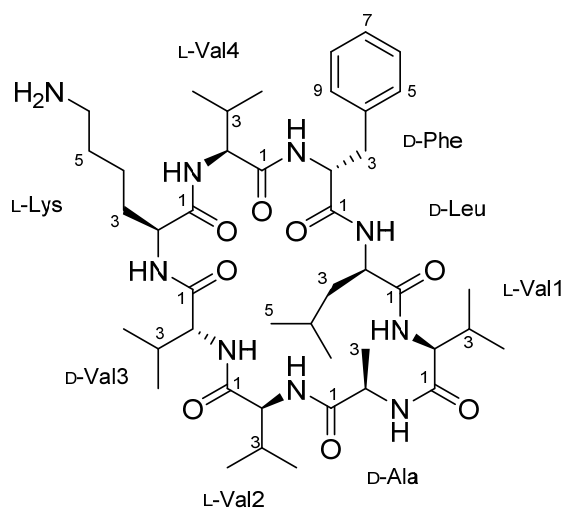


Table S7. NMR assignments for surugamide J, H, and G in CD₃OD-*d*₄. The number scheme for surugamide is shown above (Table S5).

	Position	surugamide J		surugamide H		surugamide G	
		δ_C^a	δ_H^b	δ_C^a	δ_H^b	δ_C^a	δ_H^b
Val1	1	ND		171.8		ND	
	2	60.8	4.09	60.3	4.15	61.9	3.98
	3	29.9	2.19	30.3	2.29	31.2	2.15
	4	19.9	0.97	19.7	0.96	19.8	0.98 ^c
	5	18.7	0.88	18.2	0.92	19.8	0.98 ^c
Ala	1	ND		174.9		ND	
	2	50.7	4.20	49.8	4.28	50.1	4.27
	3	18.0	1.39	19.0	1.30	18.9	1.38
Val2	1	ND		175.4		ND	
	2	63.0	3.94	61.9	3.95	61.9	3.97
	3	30.9	2.27	30.1	2.03	29.9	2.08
	4	20.6	1.05	19.7	1.05	19.8	0.98 ^c
	5	20.0	0.97	19.5	0.96	19.8	0.98 ^c
Ile1 (Val in J)	1	ND		173.8		ND	
	2	62.3	3.99	59.4	4.18	59.7	4.18
	3	31.9	2.0	37.0	2.01	37.3	1.94
	3'	-	-	14.9	0.94	15.8	0.95
	4	19.9	0.98	27.4	1.41, 1.34	27.5	1.27
Lys	5	18.9	0.97	12.1	0.91	11.8	0.91
	1	ND		ND		ND	
	2	53.0	4.53	53.1	4.45	53.2	4.46
	3	30.5	1.76	30.2	1.75	30.5	1.63
	4	23.7	1.32	25.9	1.65	25.7	1.62
	5	27.7	1.58	27.1	1.39	27.6	1.59
Val3 (Ile in G)	6	ND	2.89	40.6	2.86	40.7	2.81
	1	ND		174.3		ND	
	2	62.1	3.67	62.2	3.67	60.7	3.75
	3	30.5	1.76	30.3	1.75	36.5	1.58
	3'	-	-	-	-	15.2	0.47
Phe	4	19.7	0.83	20.1	0.85	27.5	1.31
	5	18.9	0.5	18.9	0.47	11.2	0.86
	1	ND		174.4		ND	
	2	55.7	4.7	62.2	4.6	56.3	4.62
	3	37.8	3.48, 2.73	37.5	3.46, 2.73	37.5	2.74
	4	ND		138.7		ND	
	5,9	129.7	7.25	129.7	7.28	129.9	7.28
6,8	129.9	7.26	129.5	7.27	129.8	7.27	
Leu (Val in J)	7	127.8	7.19	127.7	7.20	127.8	7.20
	1	ND		175.8		ND	
	2	59.2	4.33	54.6	4.33	54.4	4.37
	3	32.4	2.06	40.9	2.19, 1.63	40.9	2.11, 1.61
	4	19.8	0.94	26.2	1.81	26.3	1.8
	5	14.5	0.89	23.9	1.02	23.7	1.04
	6			21.4	0.94	21.7	0.97

^adetermined by edited HSQC and HMBC, ^b800 MHz, ^coverlapped signals, ND: not detected

Table S8. NMR assignments for acyl-surugamide A in DMSO-*d*₆. The number scheme for acyl-surugamide A is shown below the table.

	Position	δ_c^a	δ_H^b (Multipl., Hz)		Position	δ_c^a	δ_H^b (Multipl., Hz)
Ile1	1	169.5		Ile 4	5	28.5	1.25 (m)
	2	57.4	4.07 (m)		6	39.1	2.63 (m), 2.59 (m)
	3	35.7	1.79 (m)		NH		7.47
	3'	14.9	0.82 ^d		1	ND	
	4	25.6	1.34 (m), 1.22 (m)		2	58.0	3.8 (m)
	5	11.3	0.82 ^d		3	35.4	1.43 (m)
	NH		ND		3'	14.4	0.44 (d, 7.0)
Ala	1	172.5		4	25.7	1.34 (m), 1.23 (m)	
	2	47.9	4.26 (m)	5	10.9	0.68 (t, 7.0)	
	3	18.8	1.21 (d, 7.0)	NH		8.1	
	NH		7.79	Phe	1	170.8	
Ile2	1	ND	2		54.6	4.36 (m)	
	2	57.6	4.12 (m)		3	36.4	3.28 (m), 2.68 (m)
	3	34.8	1.76 (m)		4	137.6	
	3'	14.9	0.81 ^d		5,9	128.4	7.24 ^d
	4	24.4	1.48 (m), 1.16 (m)		6,8	129.7	7.24 ^d
	5	11.3	0.8 ^d		7	126.1	7.17 (m)
	NH		8.0 ^d	NH		8.53	
Ile3	1	ND		Leu	1	ND	
	2	56.8	4.13 (m)		2	52.6	4.18 (m)
	3	35.9	1.82 (m)		3	39.8	1.94 (m), 1.48 (m)
	3'	14.9	0.82 ^d		4	24.3	1.71 (m)
	4	25.6	1.33 (m), 1.22 (m)		5	23.1	0.96 (d, 6.5)
	5	11.3	0.82 ^d		6	21.2	0.87 (d, 6.5)
	NH		8.0 ^d		NH		7.81
Lys	1	ND		Acyl	CO	ND	
	2	51.7	4.35 (m)		2	39.9 (40.5 ^c)	2.85 (m) (2.9 ^c)
	3	31.4	1.53 (m), 1.36 (m)		3	25.7 (27.4 ^c)	1.36 (m) (1.58, 1.48 ^c)
	4	22.1	1.2 (m), 1.11 (m)		4	19.0 (20.4 ^c)	1.2 (m) (1.26 ^c)

^adetermined by edited HSQC and HMBC, ^b800 MHz, ^canalyzed in CD₃OD, ^doverlapped signals, ND: not detected

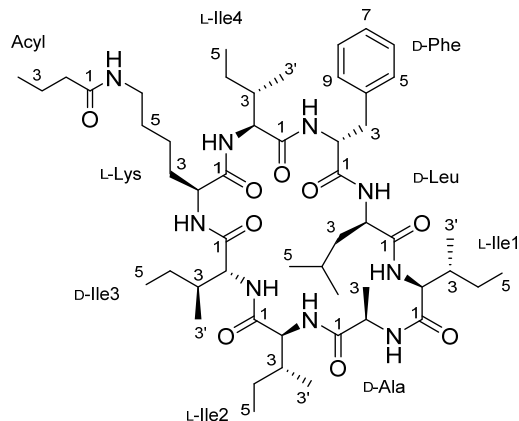


Table S9. NMR assignments for albucyclone A in DMSO-*d*₆. The numbering scheme for albucyclones is shown below the table.

	Position	δ_C^a	δ_H^b (Multipl., Hz)		Position	δ_C^a	δ_H^b (Multipl., Hz)
Ile1	1	169.8		Phe	1	ND	
	2	57.2	4.07 (m)		2	54.3	4.39 (m)
	3	36.0	1.79 (m)		3	35.6	3.25 (m), 2.68 (m)
	3'	14.8	0.81 ^c		4	138.0	
	4	23.9	1.28 (m), 1.13 (m)		5,9	128.1	7.24 ^c
	5	11.1	0.81 ^c		6,8	128.8	7.23 ^c
	NH		7.96		7	126.2	7.17 (m)
Ala	1	ND		Leu	1	ND	
	2	49.8	4.28 (m)		2	52.1	4.24 (m)
	3	18.9	1.19 (d, 7.0)		3	39.6	2.1 (m), 1.47 (m)
	NH		7.81		4	24.3	1.87 (m)
Ile2	1	ND		Iso quino ine	5	23.1	0.93 (d, 7.0)
	2	57.3	4.11 (m)		6	21.3	0.86 (d, 7.0)
	3	35.1	1.58 (m)		NH		7.78
	3'	15.0	0.71 (d, 7.0)		CO	166.9	
	4	25.5	1.13 ^c , 1.12 ^c		2	130.8	
	5	11.1	0.81 ^c		3	154.2	8.76 (s)
Ile3	1	ND		Lys	5	147.1	9.1 (s)
	2	56.5	4.09 (m)		5a	124.4	
	3	35.8	1.81 (m)		6	180.9	
	3'	14.8	0.81 ^c		7	149.3	
	4	25.5	1.13 ^c		7-NH		7.87
	5	11.1	0.81 ^c		7-NMe	28.9	2.8 (s)
	NH		7.97		8	100.5	5.64 (s)
Lys	1	ND		Ile 4	9	181.4	
	2	52.2	4.24 (m)		9a	135.7	
	3	31.5	1.58 (m), 1.45 (m)				
	4	22.2	1.25 (m), 1.19 (m)				
	5	27.9	1.45 (m), 1.37 (m)				
	6	39.0	3.30 (m), 3.08 (m)				
	6-NH		8.18				

^adetermined by edited HSQC and HMBC, ^b800 MHz, ^coverlapped signals, ND: not detected

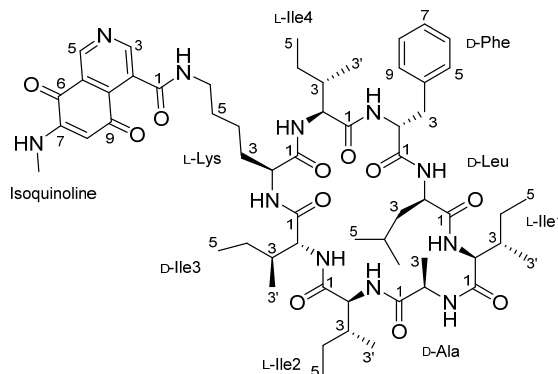


Table S10. NMR assignments of albucyclone F in CD₃OD.

	Position	δ_C^a	δ_H^b		Position	δ_C^a	δ_H^b
Val1	1	174.7		Val4	1	ND	
	2	60.0	4.23		2	62.1	3.69
	3	31.1	2.22		3	30.2	1.78
	4	19.6	0.99		4	19.7	0.88
	5	18.5	0.97 ^c		5	18.9	0.51
Ala	1	175.3		Phe	1	ND	
	2	50.3	4.31		2	55.8	4.7
	3	18.1	1.35		3	37.5	3.49, 2.73
4	174.0		4		138.6		
Val2	1	174.0		5, 9	129.3	7.28	
	2	61.2	4.00	6, 8	129.9	7.28	
	3	29.8	1.97	7	127.6	7.21	
	4	20.0	0.89	Leu	1	ND	
	5	19.8	0.95 ^c		2	54.5	4.42
Val3	1	173.2			3	40.9	2.12, 1.58
	2	61.5	4.03		4	26.1	1.82
	3	31.6	2.09		5	23.6	1.02
	4	19.8	0.95 ^c	6	21.5	0.97	
	5	19.8	0.95 ^c	Isoquinoline	CO	169.7	
Lys	1	ND			2	131.7	
	2	ND	4.01		3	154.8	8.83
	3	32.9	1.31		5	148.7	9.21
	4	23.9	1.44		5a	126.2	
	5	29.0	1.64, 1.56		6	181.3	
	6	40.4	3.61, 3.22		7	150.7	
			7-NMe		29.1	2.93	
			8		101.3	5.81	
			9	181.7			

^adetermined by edited HSQC and HMBC, ^b800 MHz, ^coverlapped signals, ND: not detected

Table S11. NMR assignments for albucyclone D and E in CD₃OD.

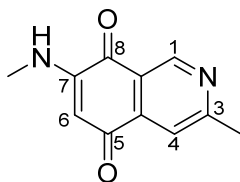
albucyclone D				albucyclone E			
	Position	δ_C^a	δ_H^b		Position	δ_C^a	δ_H^b
Val1	1	ND		Val1	1	ND	
	2	59.8	4.22		2	59.9	4.22
	3	30.0	1.92		3	31.2	2.18
	4	19.6	0.97		4	19.5	0.97
	5	19.6	0.95 ^c		5	19.5	0.95 ^c
Ala	1	ND		Ala	1	ND	
	2	50.2	4.28		2	50.0	4.28
	3	18.8	1.34		3	18.6	1.33
Val2	1	ND		Ile1	1	ND	
	2	61.7	4.01		2	60.2	3.75
	3	31.6	2.08		3	36.4	1.72
	4	19.6	0.95 ^c		3'	15.9	0.80
	5	18.5	0.93		4	24.1	1.20
Ile1	1	ND		Val2	5	11.6	0.86
	2	60.2	4.03		1	ND	
	3	36.4	1.72		2	61.3	3.99
	3'	15.9	0.80		3	30.1	1.95
	4	24.1	1.20		4	19.8	0.86
Lys	5	11.6	0.86	Lys	5	19.4	0.95
	1	ND			1	ND	
	2	53.9	4.46		2	53.6	4.46
	3	32.7	1.68		3	ND	1.68
	4	23.8	1.44		4	23.9	1.42
	5	28.9	1.61		5	28.8	1.63
Val3	6	ND		Val3	6	ND	
	1	ND			1	ND	
	2	62.0	3.66		2	61.8	3.67
	3	30.3	1.77		3	30.1	1.76
	4	18.9	0.85		4	20.0	0.85
Phe	5	19.0	0.47	Phe	5	19.0	0.48
	1	ND			1	ND	
	2	55.9	4.65		2	55.8	4.66
	3	37.5	3.47, 2.74		3	37.1	3.47, 2.73
	4	ND			4	ND	
	5,9	129.4	7.26		5,9	129.4	7.26
	6,8	129.9	7.26		6,8	129.7	7.26
7	127.7	7.19	7	127.5	7.20		
Leu	1	ND		Leu	1	ND	
	2	54.5	4.41		2	54.1	4.39
	3	40.9	2.10, 1.56		3	40.8	2.10, 1.56
	4	25.8	1.81		4	25.9	1.80
	5	23.9	1.01		5	23.6	1.01
	6	21.5	0.96		6	21.3	0.95
N-Me		29.5	2.91	N-Me		29.0	2.91

^adetermined by edited HSQC and HMBC, ^b800 MHz, ^coverlapped signals, ND: not detected

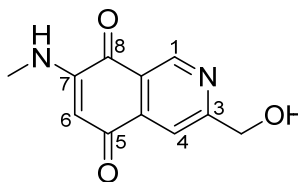
Table S12. NMR assignments of albuquinone A in DMSO- d_6 and 3-methyl-7-(methylamino)-5,8-isoquinolinedione and in CD $_3$ OD. The numbering schemes for both compounds are shown below the table.

3-methyl-7-(methylamino)-5,8-isoquinolinedione			albuquinone A		
No.	δ_c^a	δ_H^b (Multipl., Hz)	No.	δ_c^a	δ_H^b (Multipl., Hz)
1	147.7	9.03 (s)	1	146.36	9.02 (s)
3	167.6		3	170.4	
3-Me	24.8	2.67 (s)	3 α ,3 β	64.6	4.68 (s)
4	119.7	7.81 (s)	4	114.3	7.92 (s)
4a	141.3		4a	140.0	
5	182.0		5	180.1	
6	100.3	5.77 (s)	6	99.6	5.71 (s)
7	152.2		7	150.3	
8	181.1		8	181.2	
8a	124.0		8a	123.7	
N-Me	29.6	2.93 (s)	N-Me	28.8	2.81 (s)

^adetermined by edited HSQC and HMBC, ^b500 MHz



3-methyl-7-(methylamino)-5,8-isoquinolinedione



albuquinone A

Figure S1. Genotype validation of three double crossover mutants, $\Delta surA$ (A), $\Delta surB$, and $surE::eGFPx3$. Primers used for validation are shown in Table S2. See SI Methods for a detailed description of the construction strategies used.

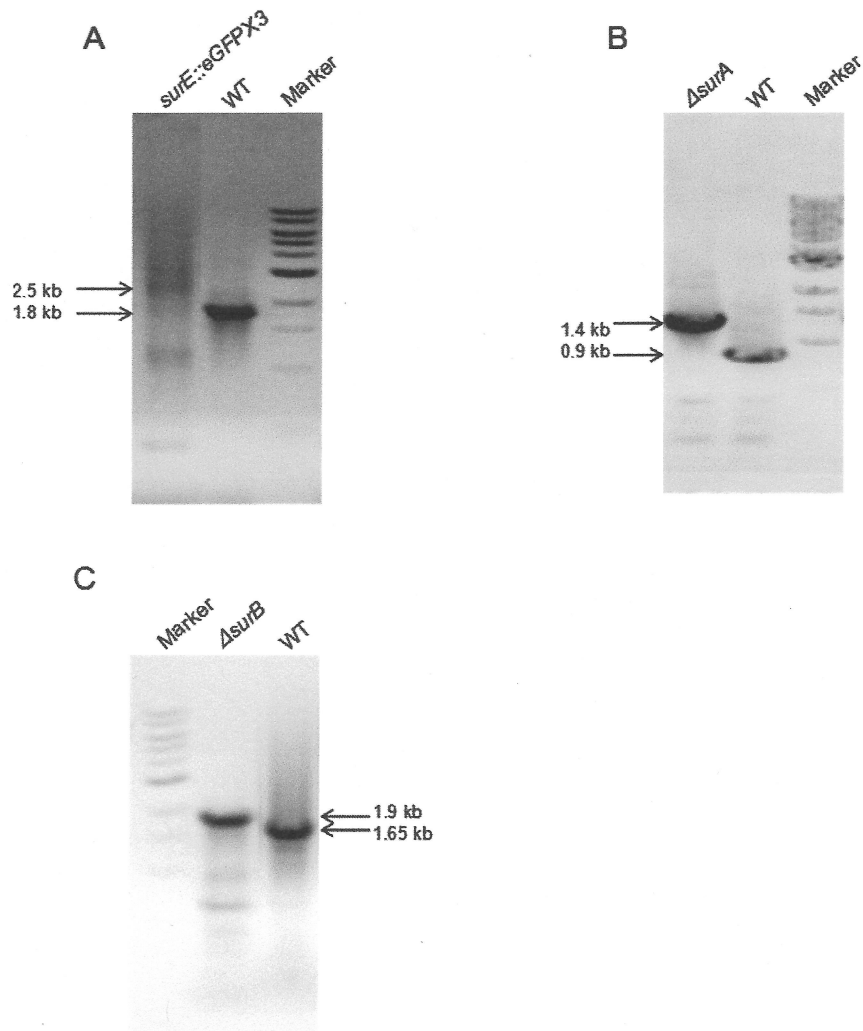


Figure S2. Analysis of RNA integrity used for qPCR experiments. Agarose gels of total RNA isolated from wt *S. albus* J1074 cultures after treatment with DMSO control and small molecule elicitors. Shown are RNA samples used for main text Fig. 3B (A), Fig. 3C (B), and Fig. 5A (C). The abbreviations are as follows: Bro, 6-bromolaudanosine; Cyc, cyclosporin; Dhe, dihydroergocristine; Eto, etoposide; Ive, ivermectin; Pic, piceatannol. For etoposide and ivermectin, 1X concentration corresponds to 5.7 μ M and 7.6 μ M, respectively.

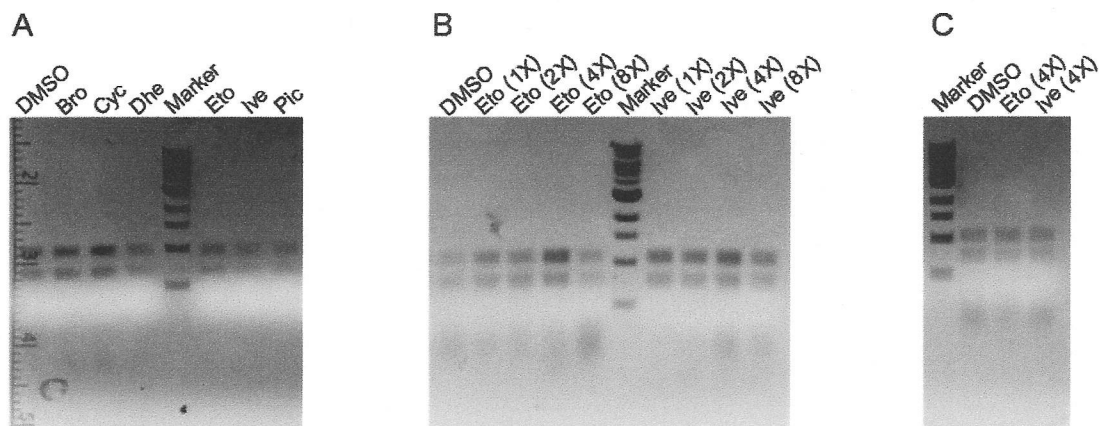


Figure S3. Detection of the products of the *sur* cluster in wt *S. albus* J1074 as well as $\Delta surA$ and $\Delta surB$ knockout strains in the presence and absence of etoposide or ivermectin. Shown are extracted ion chromatograms for surugamides (A), acyl-surugamides (B), albucyclones (C), and surugamide F-F3 (D). In each panel the variants, denoted by upper-case letters, are marked. Note that surugamide F requires *surB* but not *surA*, while all other surugamides require *surA* but not *surB*. Thus, the *sur* cluster gives rise to two different natural product scaffolds. The traces in all panels have been off-set in the y-axis (MS intensity) for clarity.

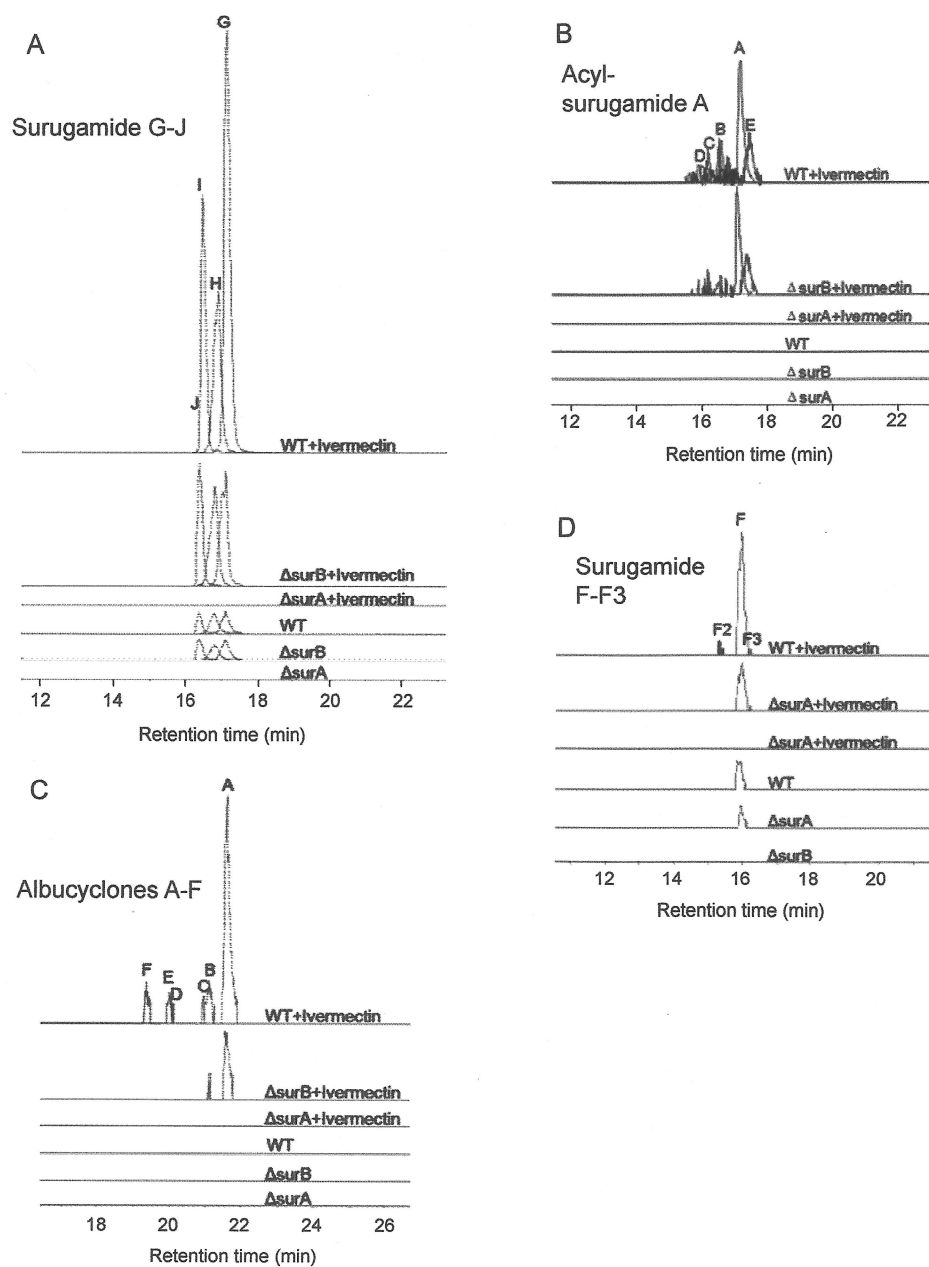


Figure S4. UV-visible absorption spectra for each category of compounds purified from *S. albus* J1074. Shown are spectra for surugamide I (A), acyl-surugamide A (B), albucyclone A (C), surugamide F (D) and albuquinone A (E).

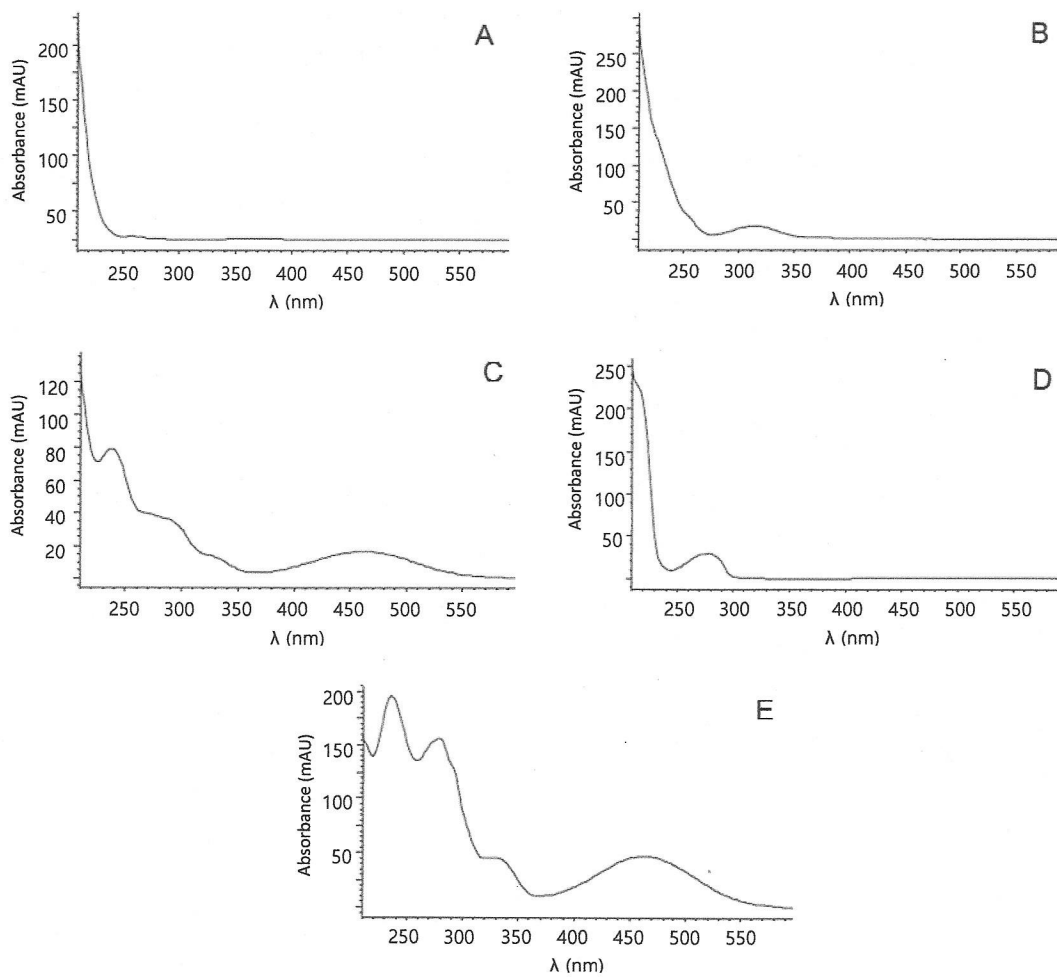
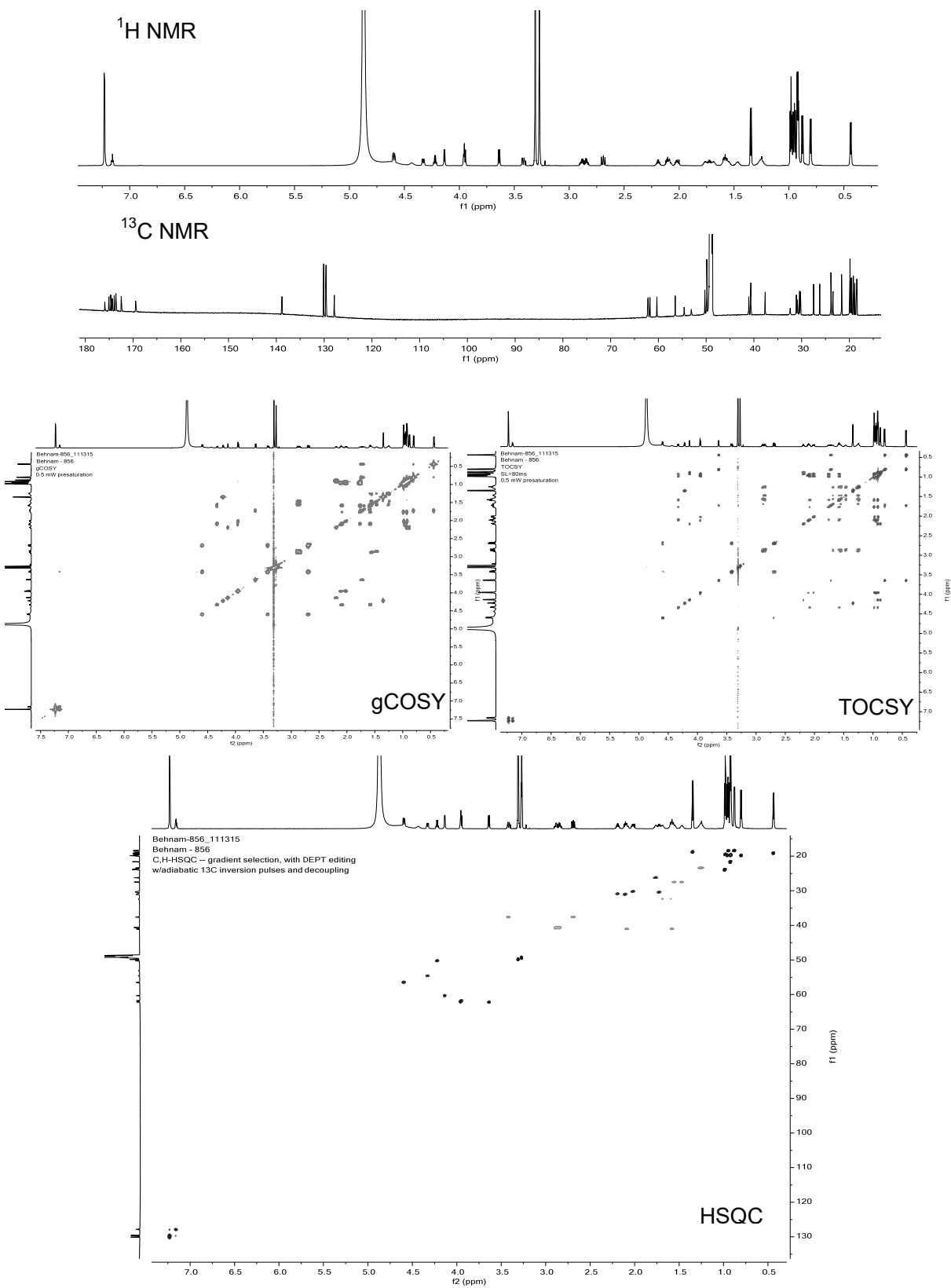


Figure S5. NMR spectra (800 MHz) of surugamide I in CD₃OD (pages S27-S28).



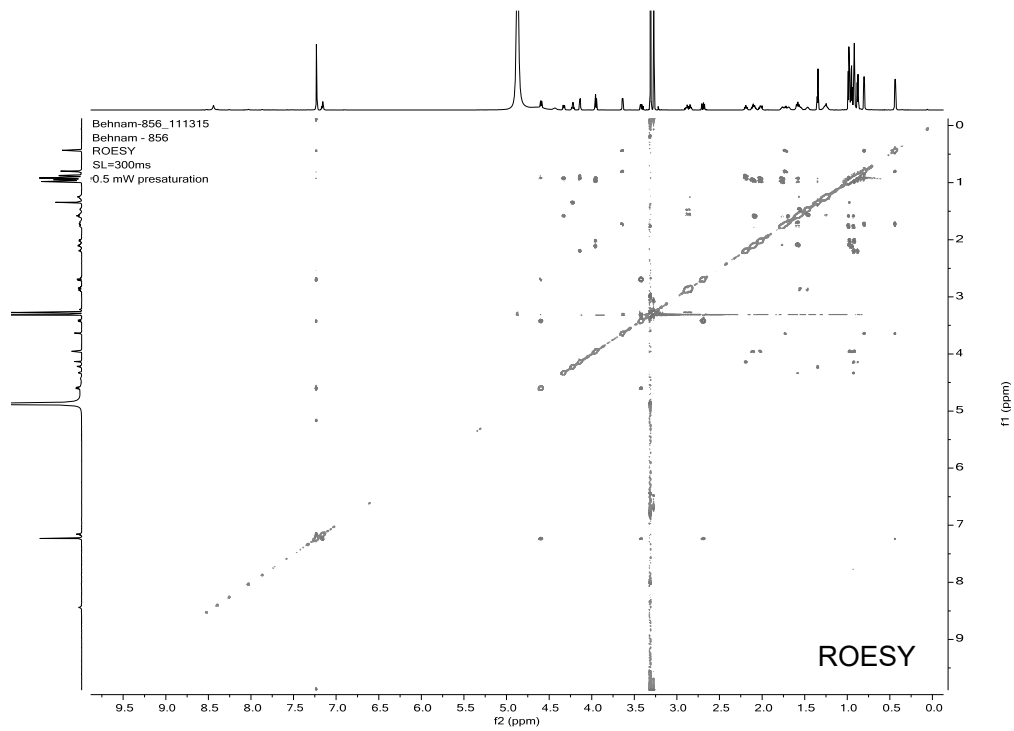
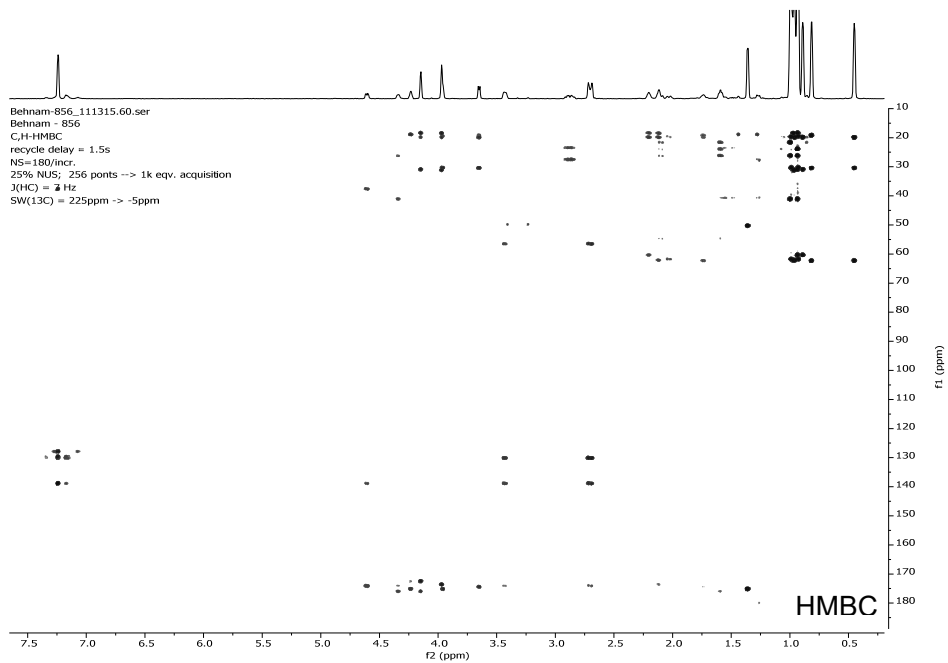


Figure S6. NMR spectra (800 MHz) of surugamide J in CD₃OD.

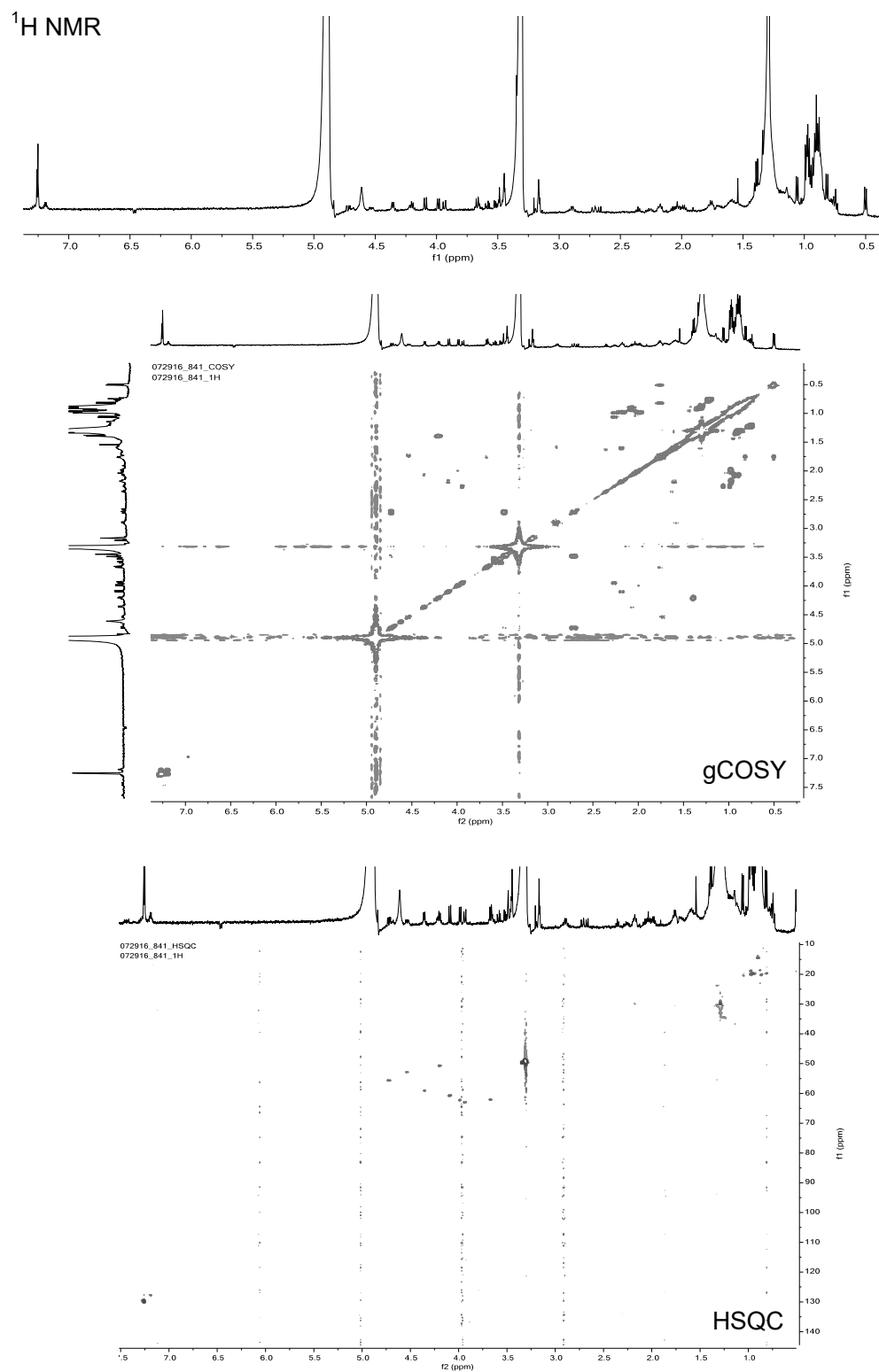
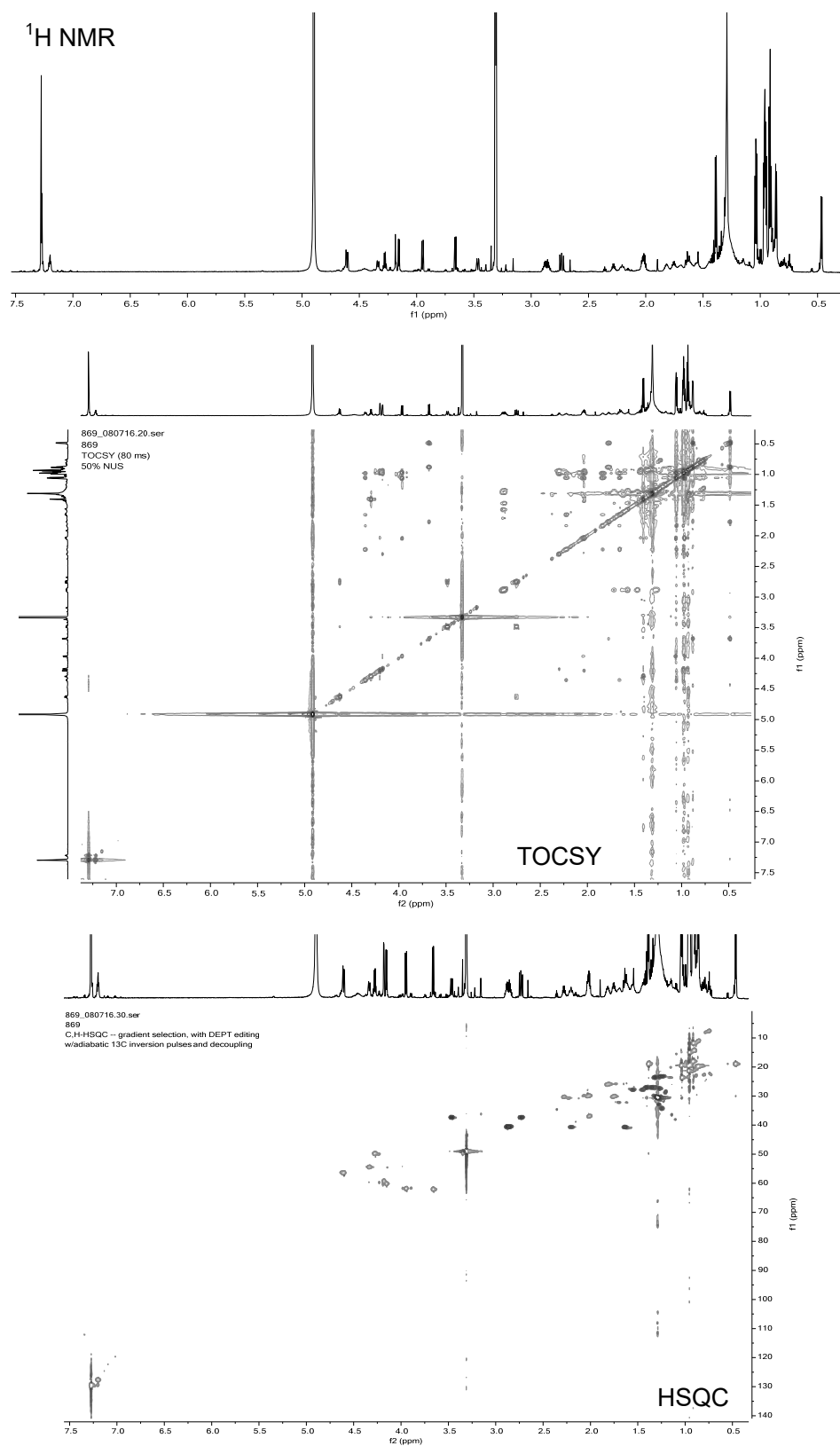


Figure S7. NMR spectra (800 MHz) of surugamide H in CD₃OD (pages S30-S31).



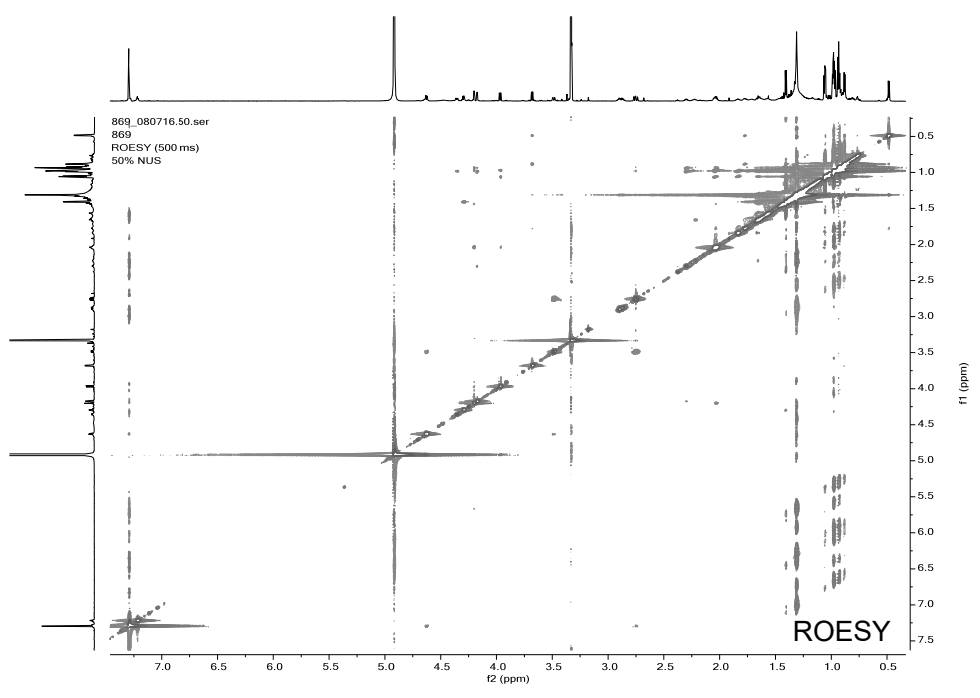
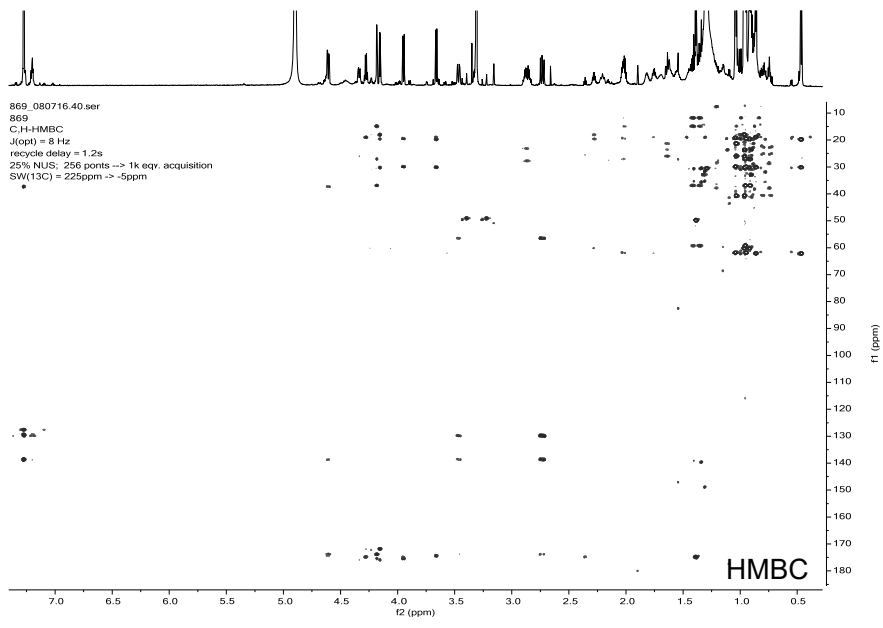


Figure S8. NMR spectra (500 MHz) of surugamide G in CD₃OD.

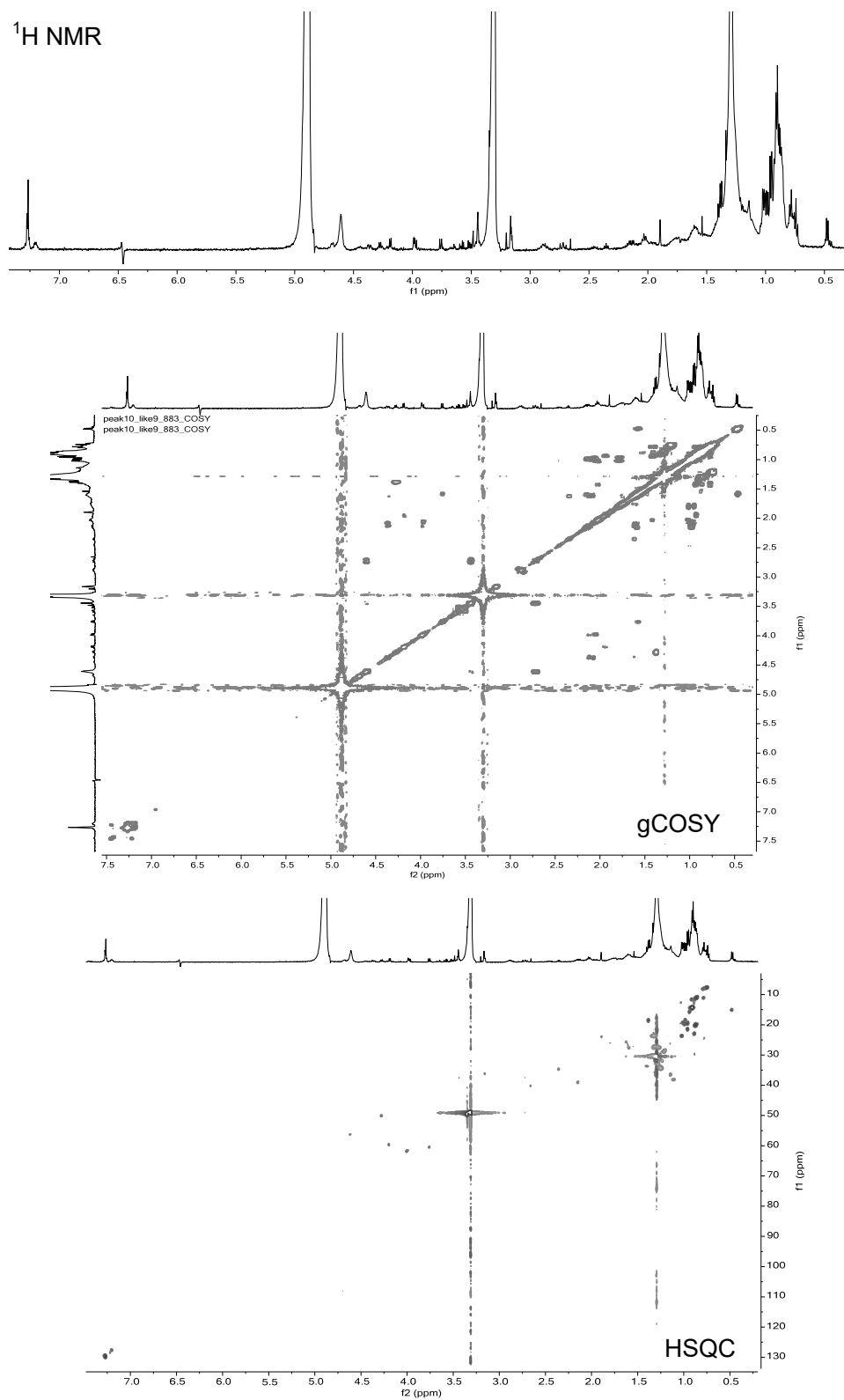
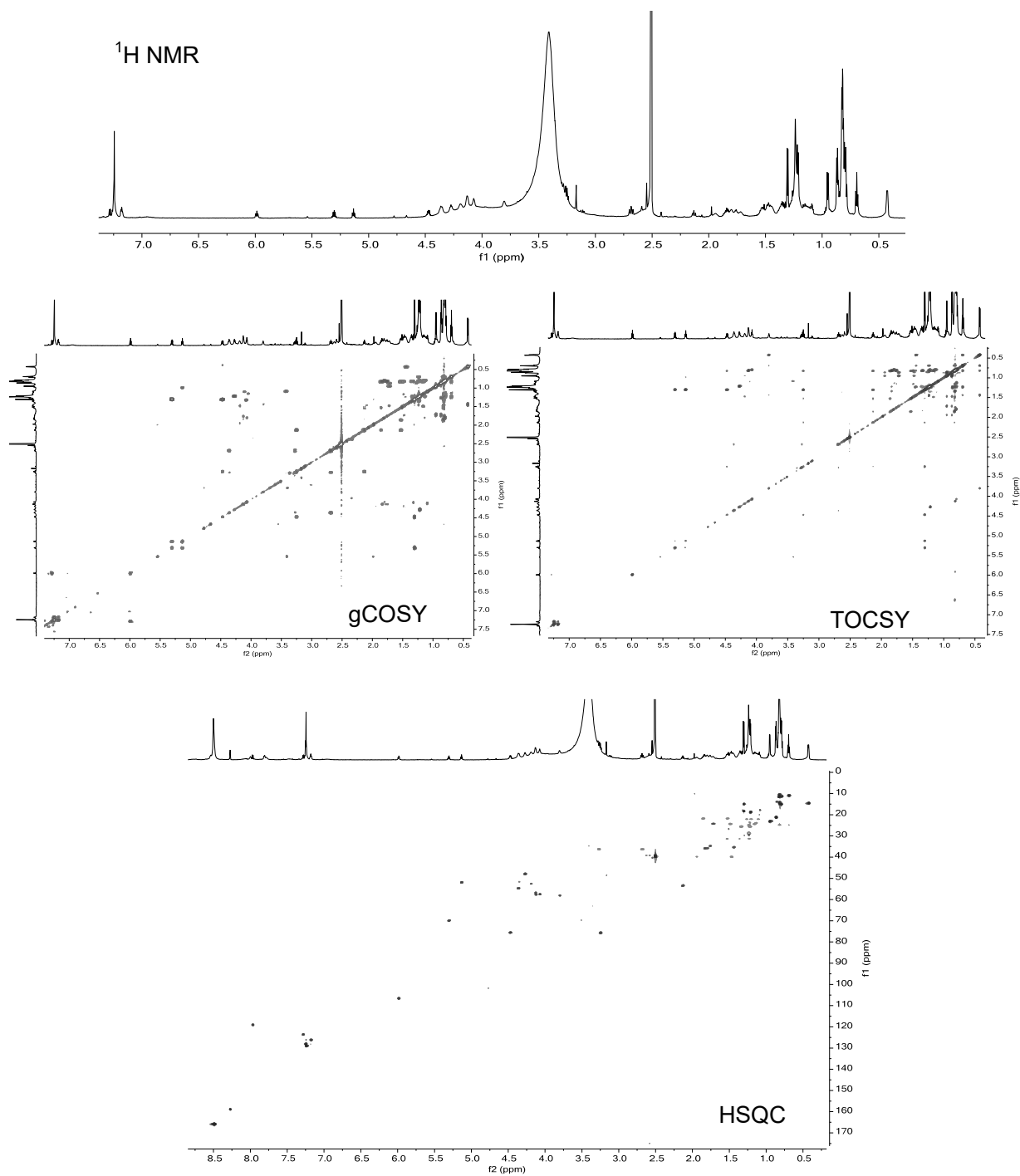


Figure S9. NMR spectra (800 MHz) of acyl-surugamide A in DMSO-d₆ (pages S33-S34). Note that peaks between 5–6 ppm are associated with impurities.



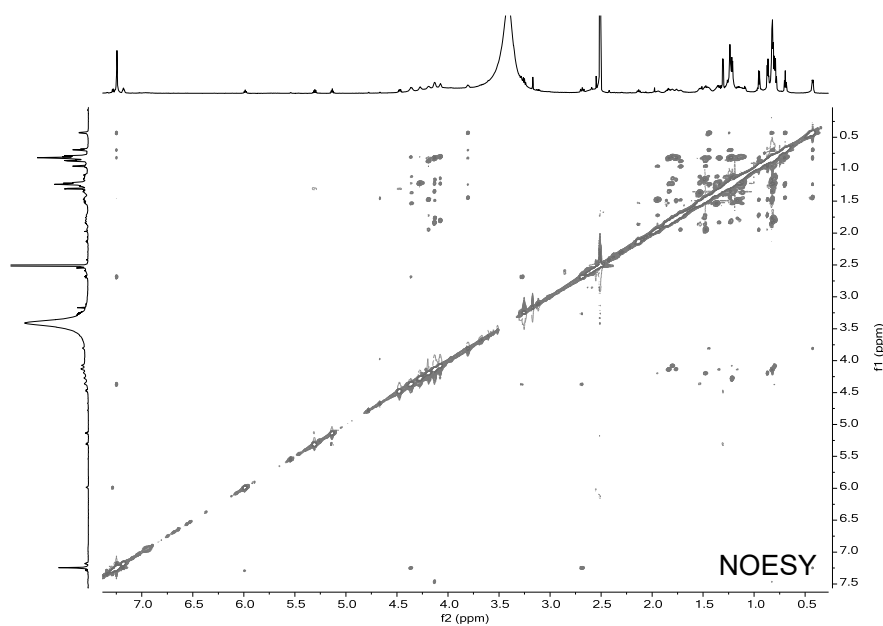
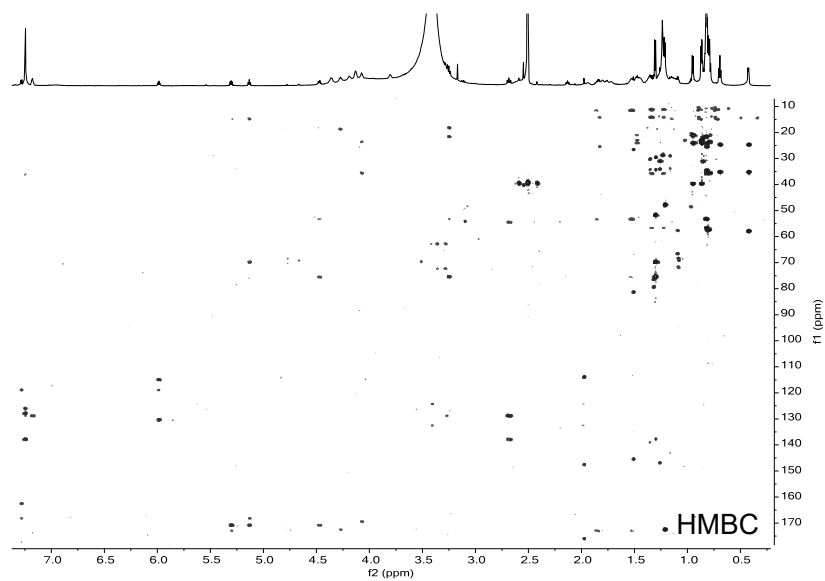


Figure S10. Additional evidence for the acyl group in acyl-surugamide A. (Top) NOESY spectrum of acyl-surugamide A in DMSO- d_6 . The CH₂ group alpha to the carbonyl group of the acyl chain is boxed. The ¹³C-shift for this methylene group is shown in the HSQC spectrum (middle). (Bottom) TOCSY spectrum of acyl-surugamide A in CD₃OD. The CH₃-CH₂-CH₂ correlation of the acyl group is boxed. Correlations for acyl-surugamide A are pointed out. The acyl-to-lysine cross-peak was observed in NOESY spectra in CD₃OD and in DMSO- d_6 .

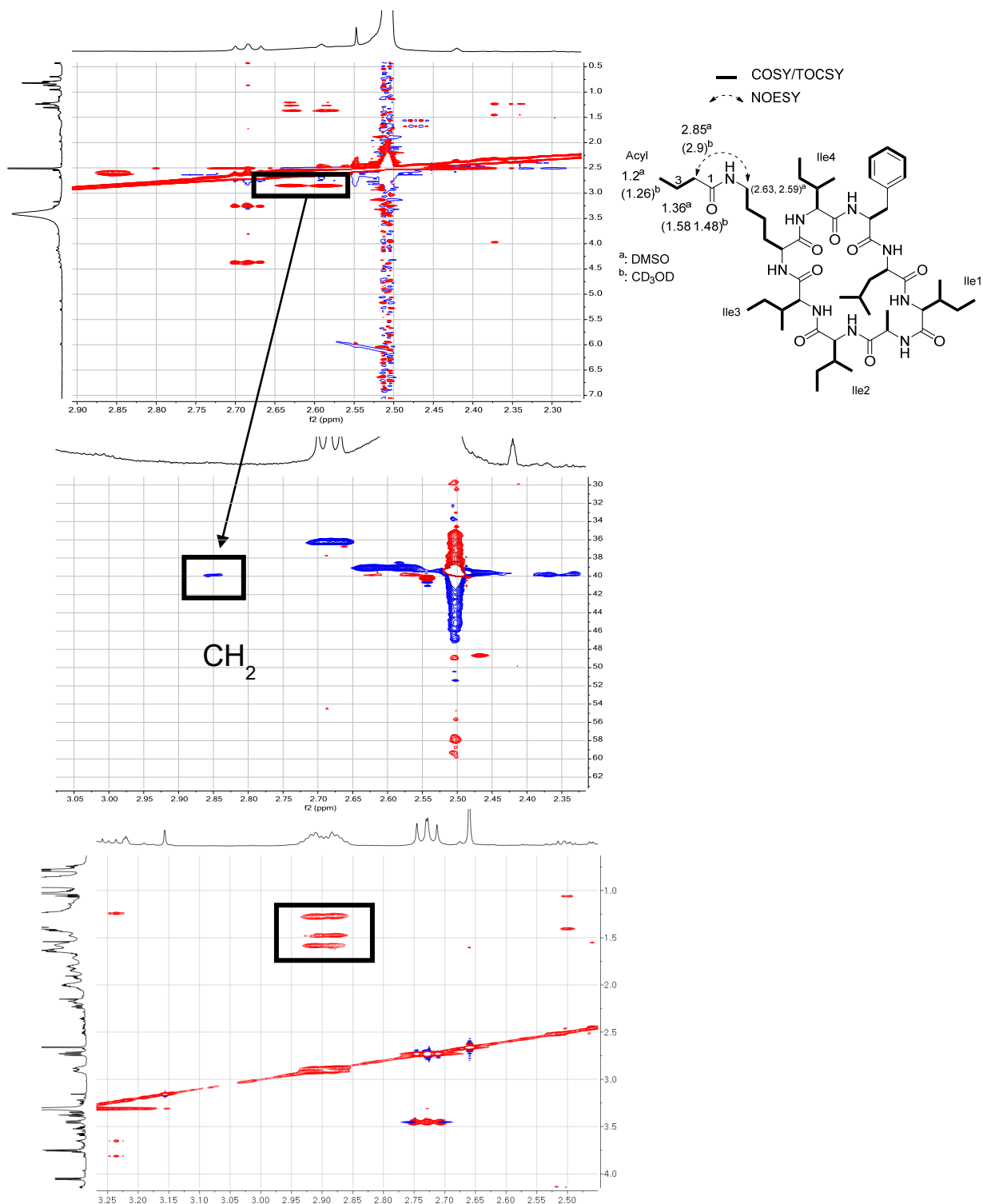
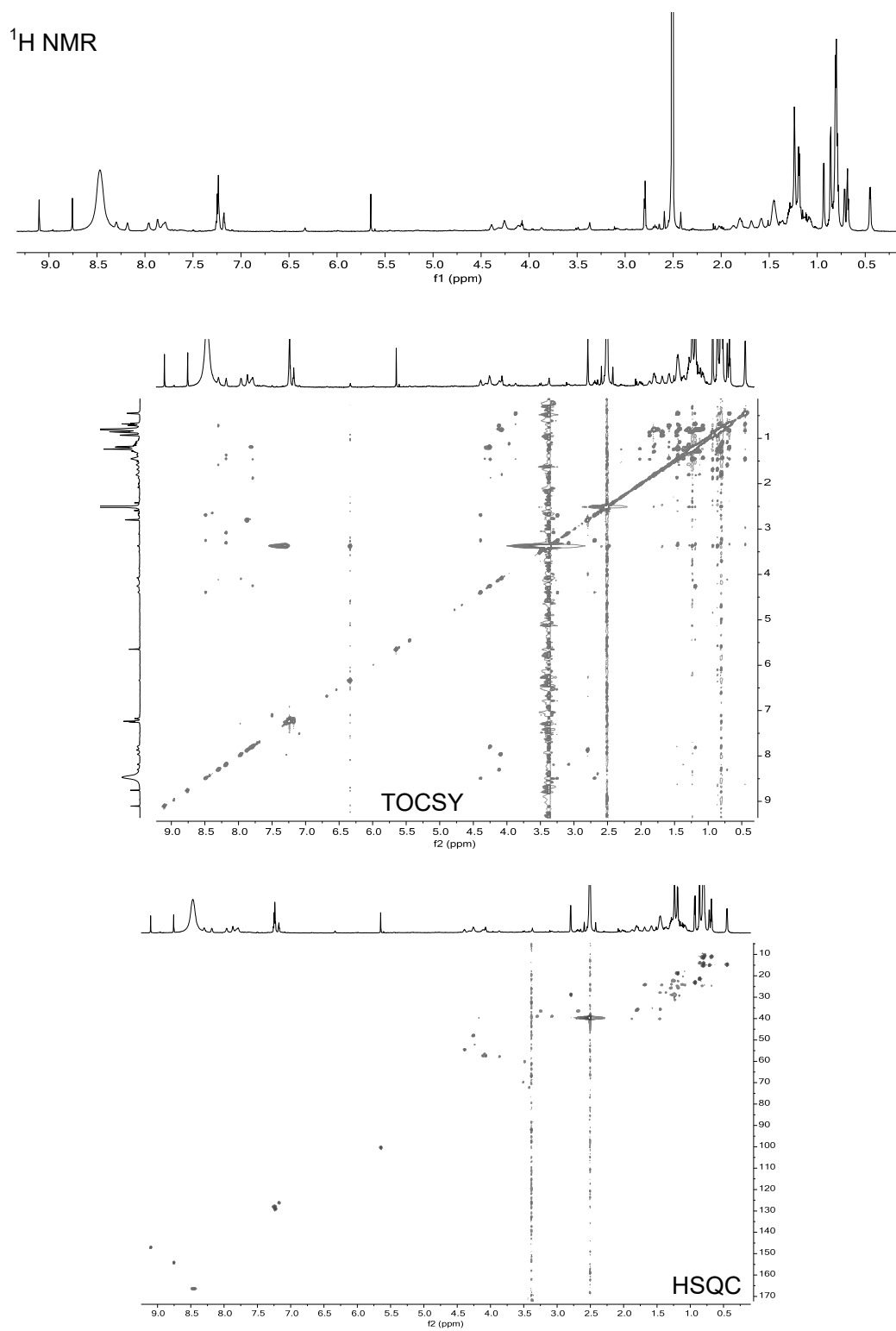


Figure S11. NMR spectra (800 MHz) of albucyclone A in DMSO-*d*₆ (pages S36-S37).



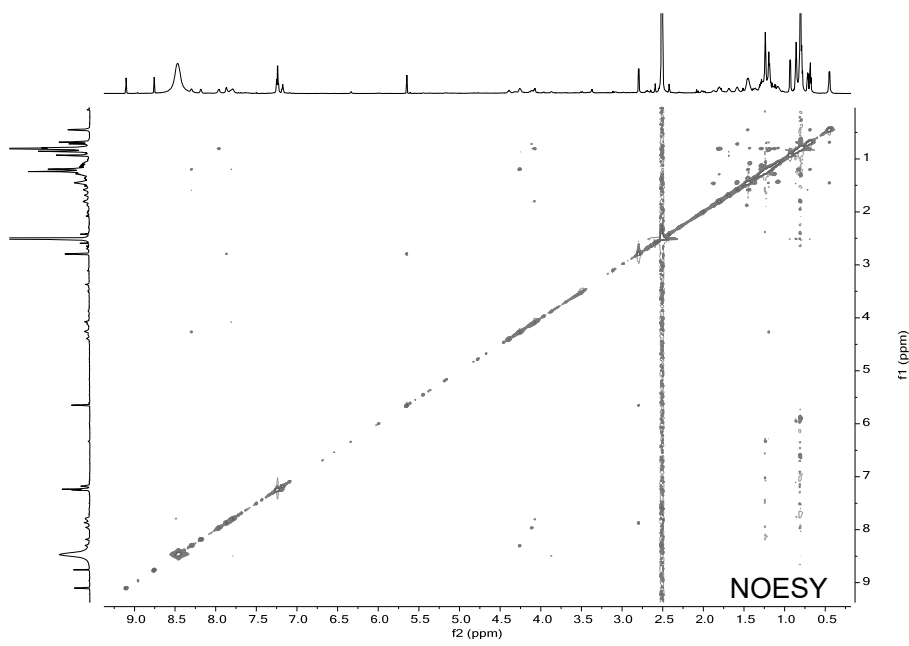
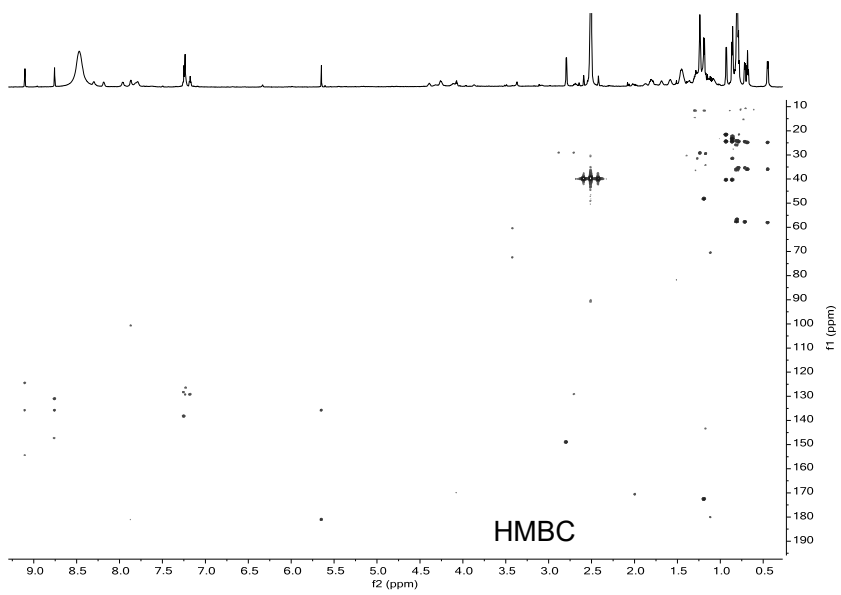


Figure S12. Additional evidence for attachment of the quinone moiety to the lysine sidechain in albucyclones A. (Top) TOCSY spectra (800 MHz, DMSO- d_6) show correlation between the lysine amide proton and the rest of the lysine sidechain (boxed). (Bottom) This amide proton shows an HMBC correlation to the same carbonyl group (the amide-carbonyl) as the C3-proton on the quinone sidechain (8.76 ppm). See Table S8 and Scheme 1 in the main text.

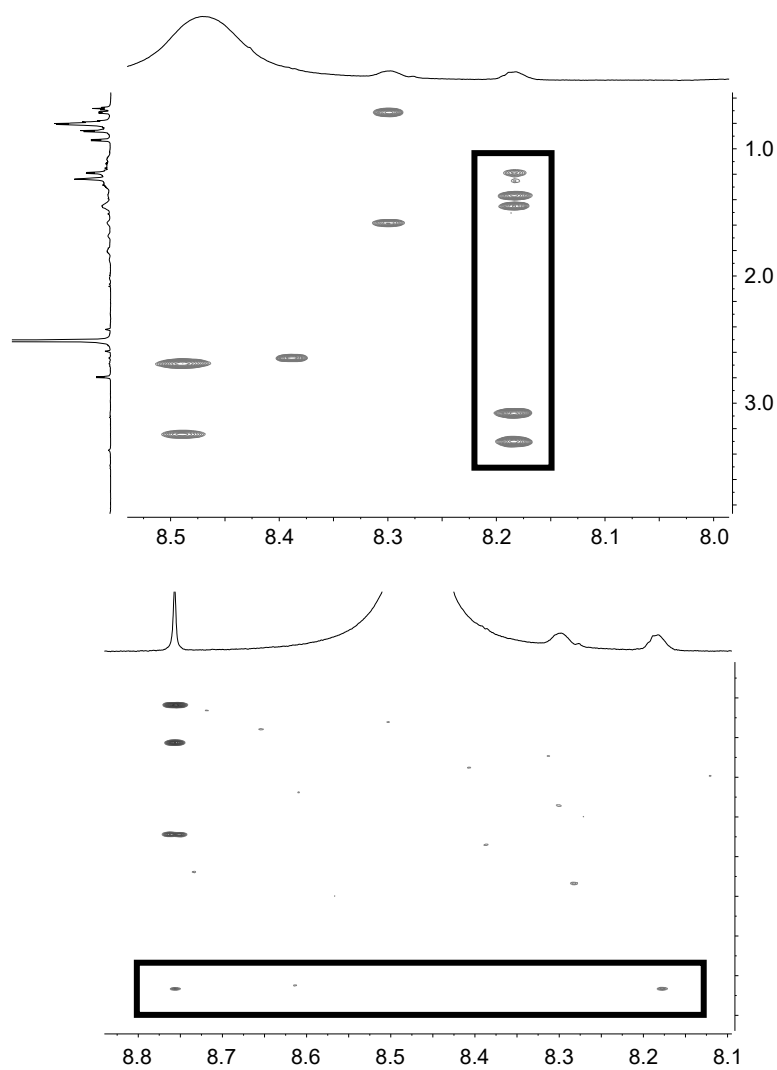
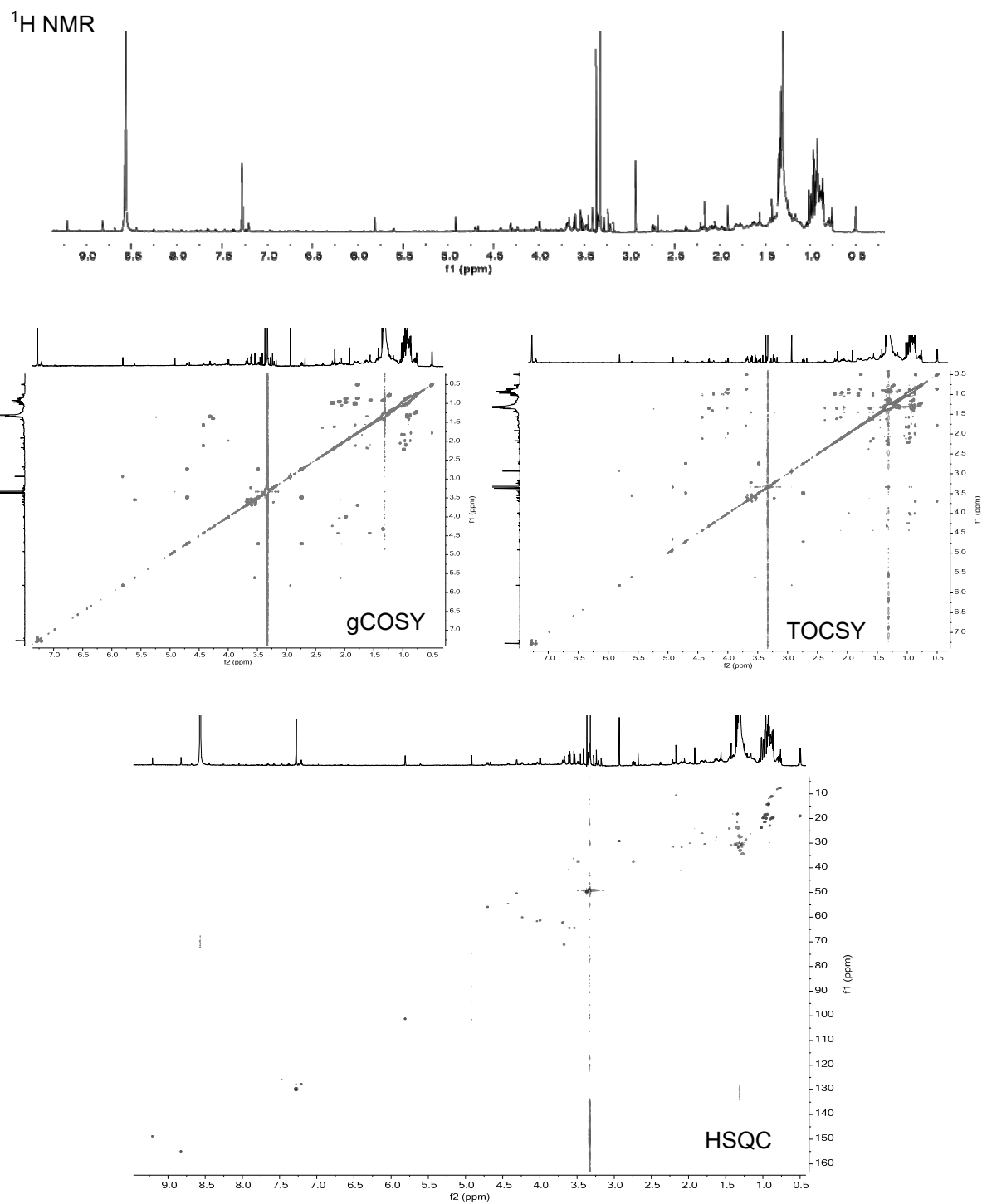


Figure S13. NMR spectra (800 MHz) of albucyclone F in CD₃OD-*d*₄ (pages S39-S40).



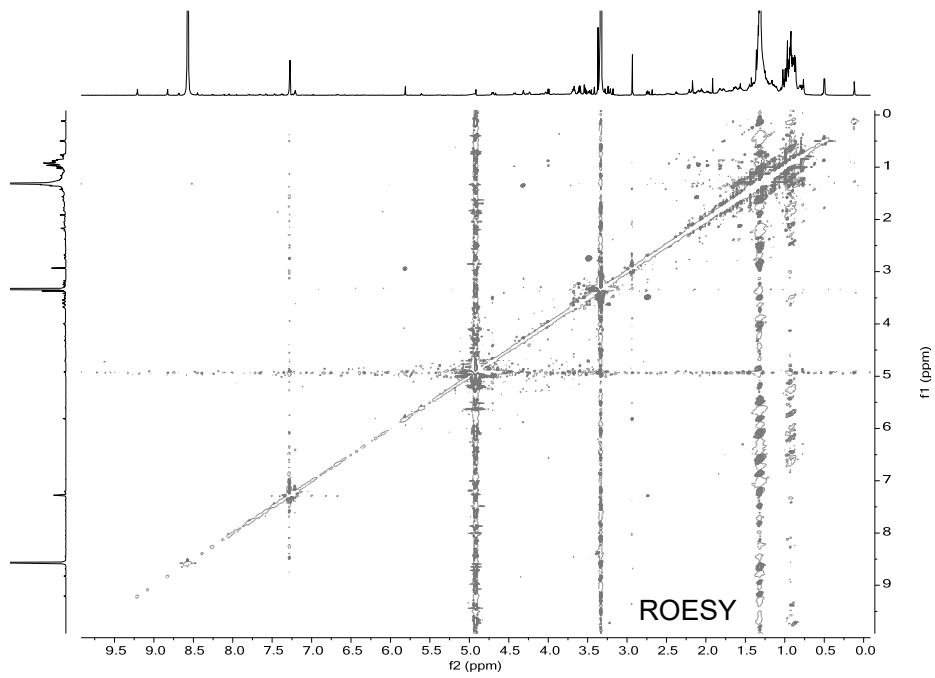
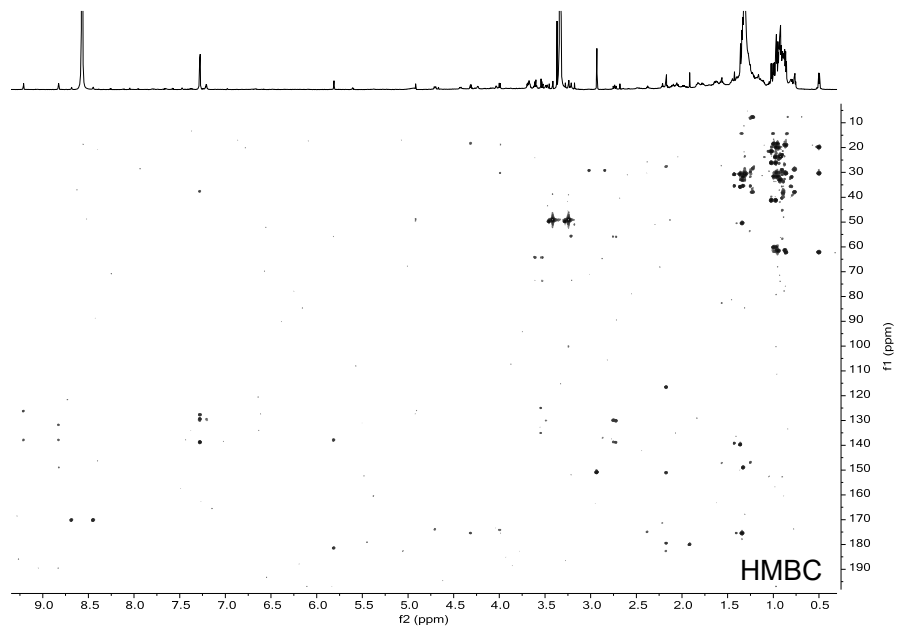


Figure S14. HR-MS/MS fragmentation analysis of albucyclone B.

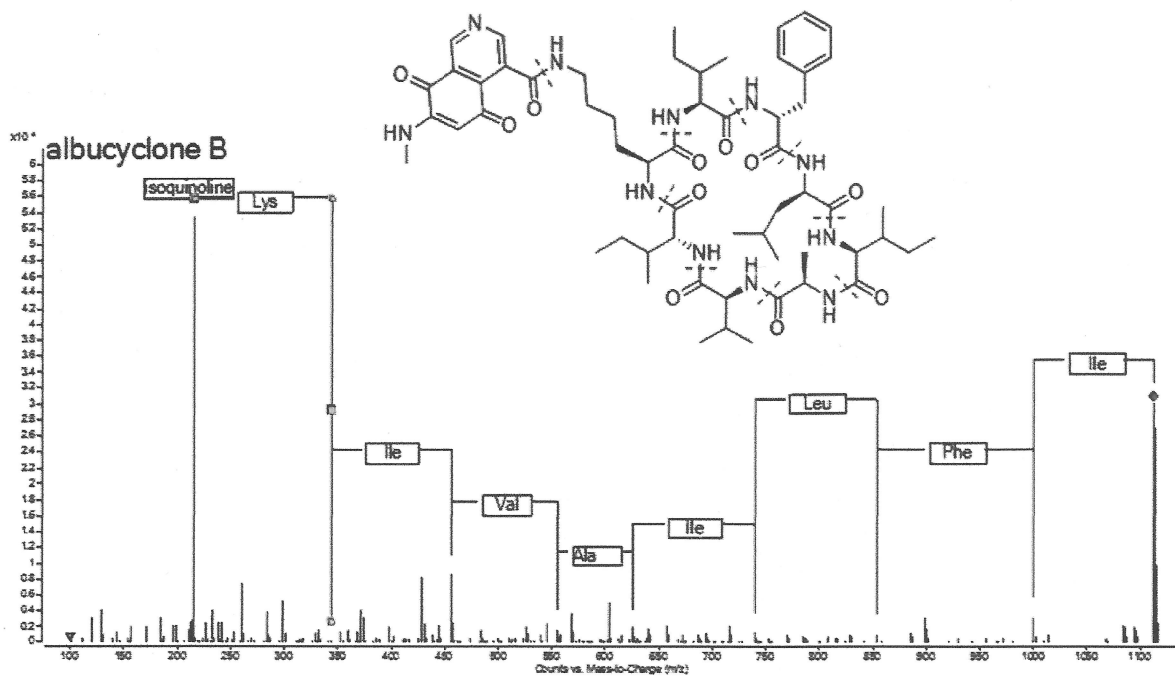


Figure S15. HR-MS/MS fragmentation analysis of albucyclone C.

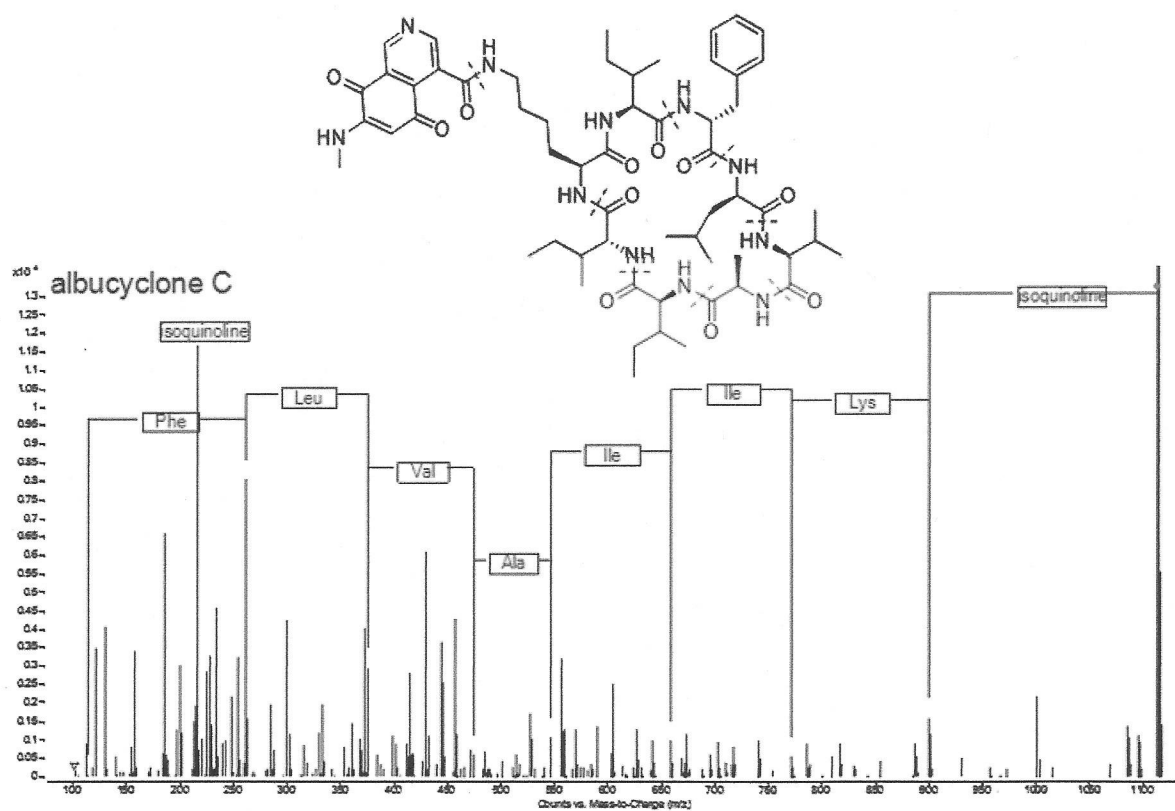
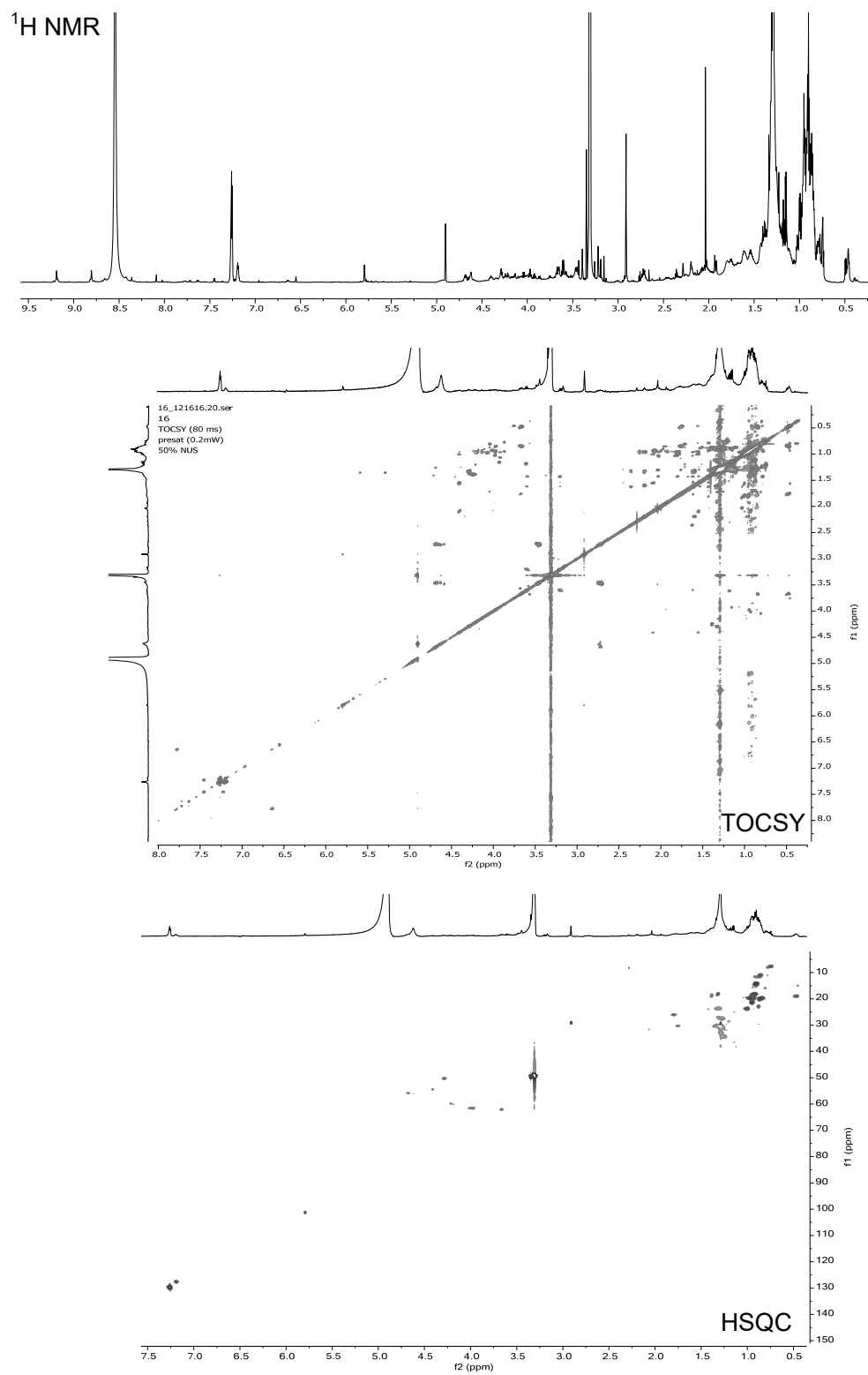


Figure S16. NMR spectra (800 MHz) and HR-MS/MS fragmentation analysis of albucyclone D in CD₃OD (pages S43-S44).



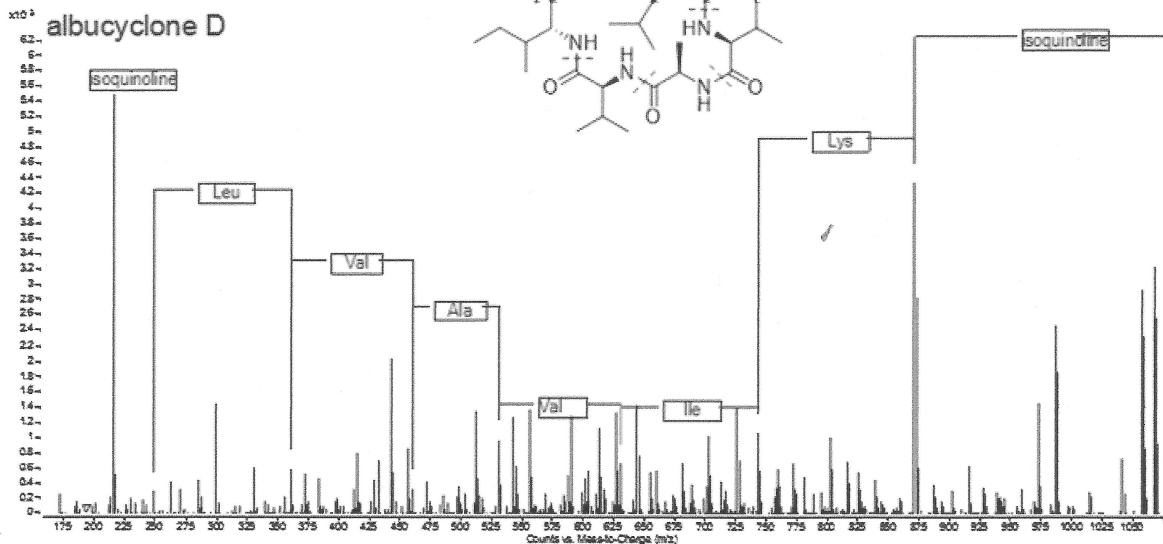
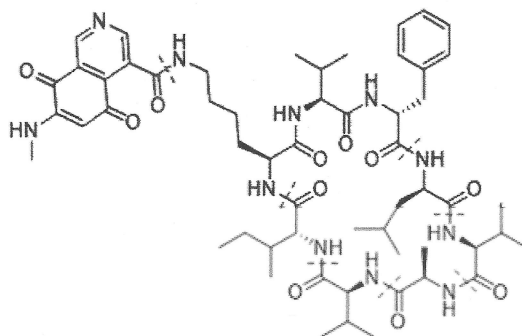


Figure S17. HR-MS/MS fragmentation analysis of albucyclone E.

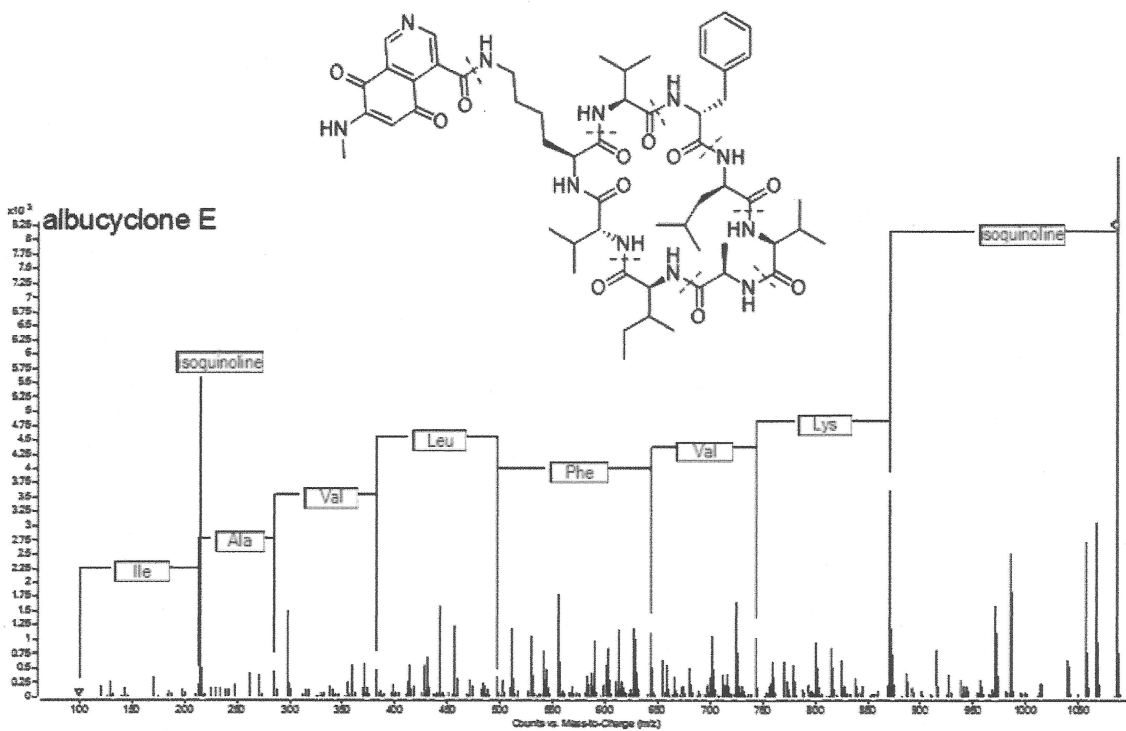


Figure S18. NMR spectra (500 MHz) of albuquinone A in DMSO- d_6 . Shown are ^1H (top), HSQC (middle) and HMBC (bottom) spectra. See Scheme 1 in the main text.

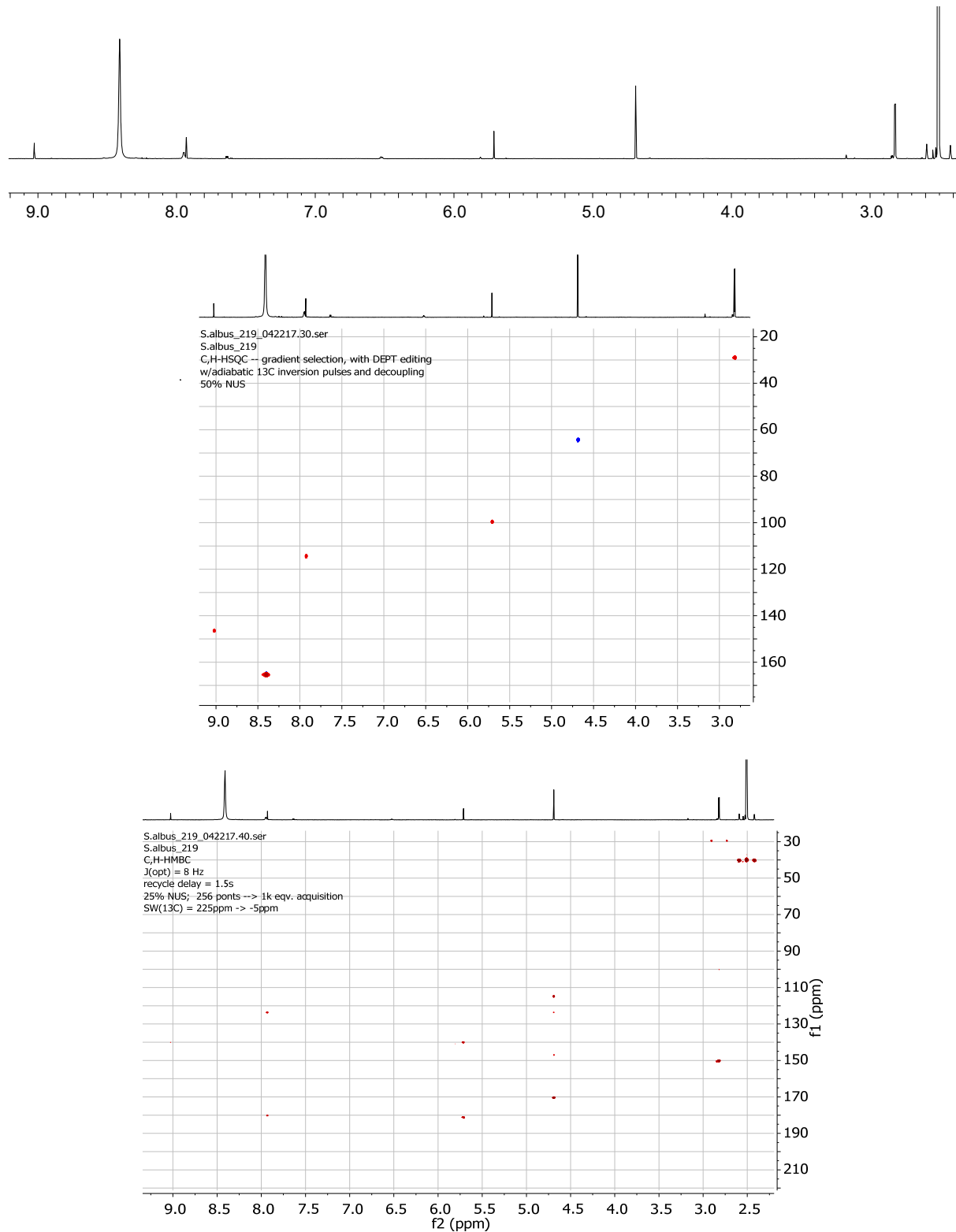


Figure S19. HR-MS/MS analysis of surugamide F2 compared with surugamide F.

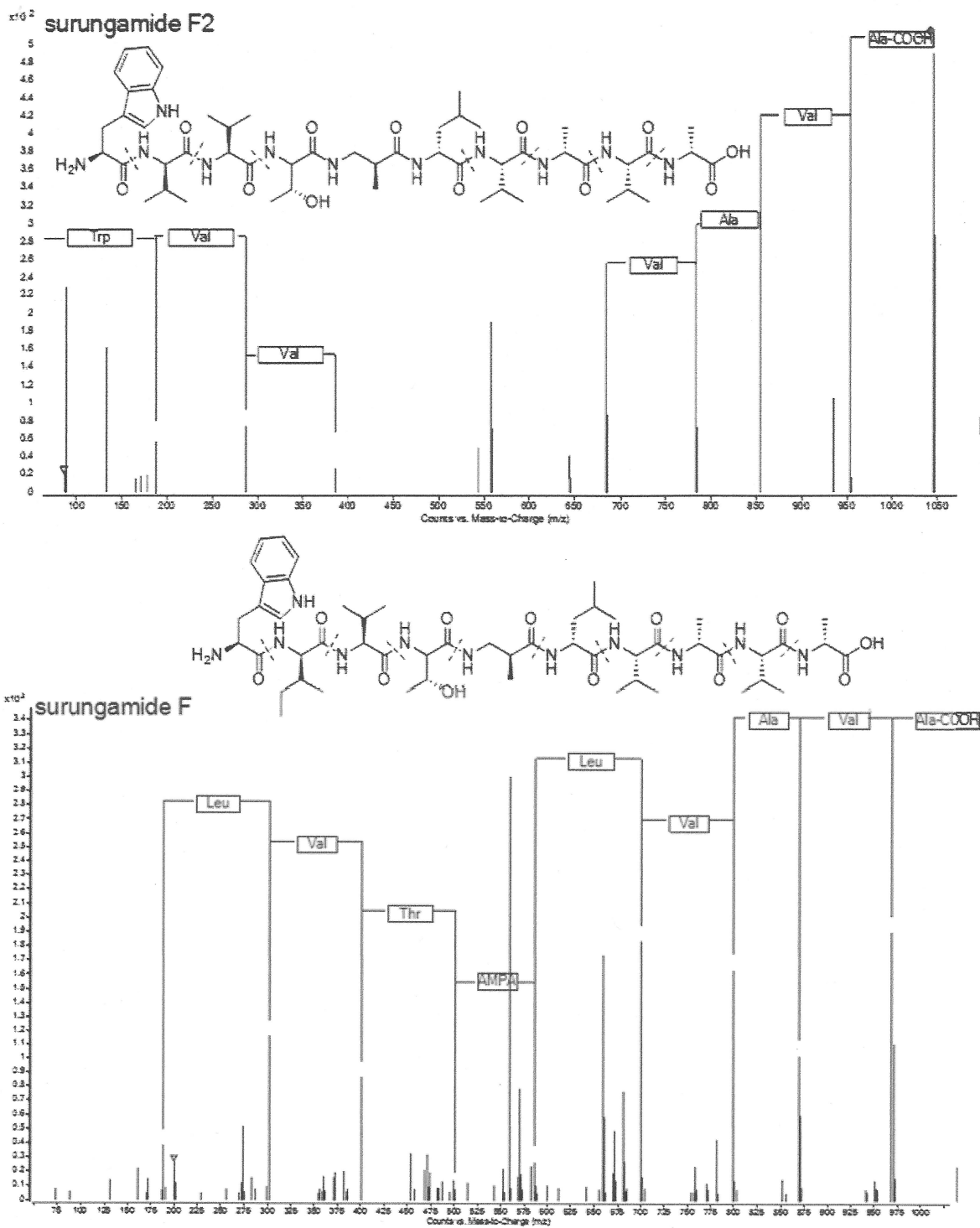


Figure S20. HR-MS/MS analysis of surugamide F3 compared with surugamide F.

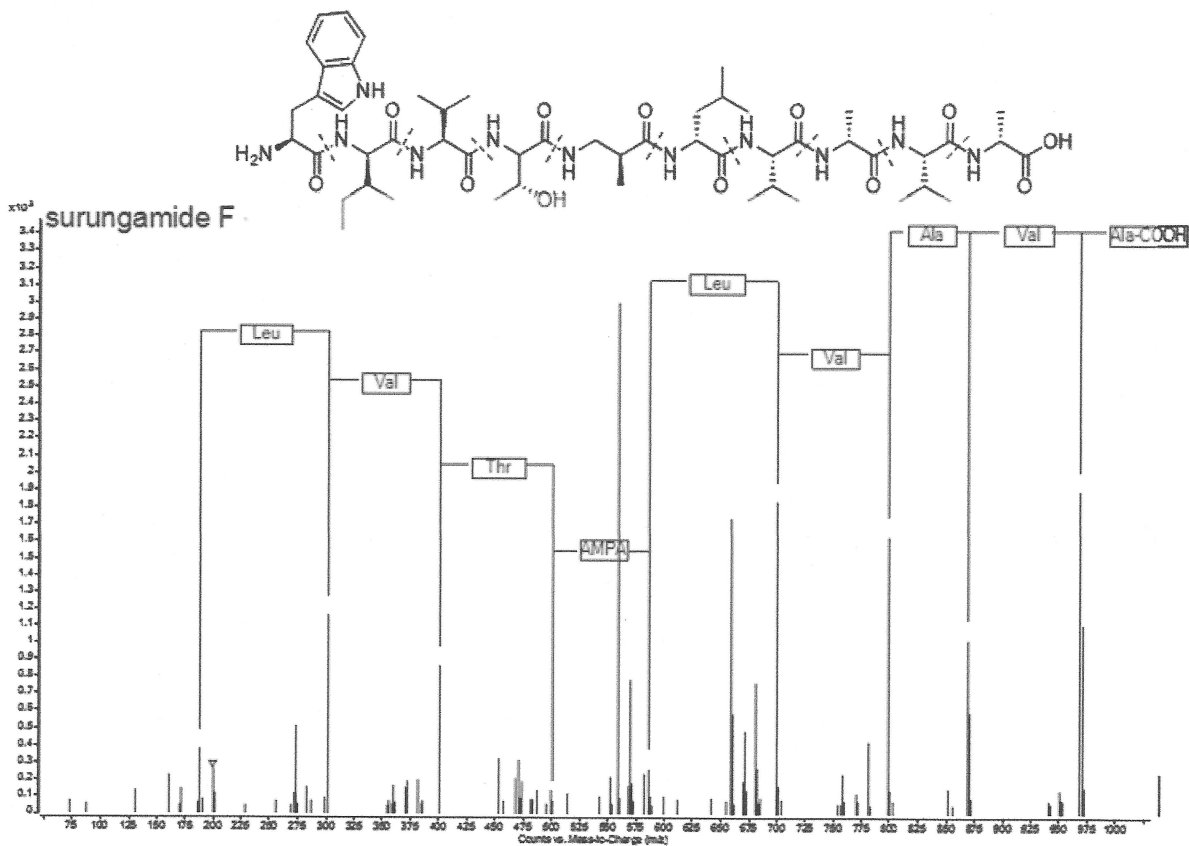
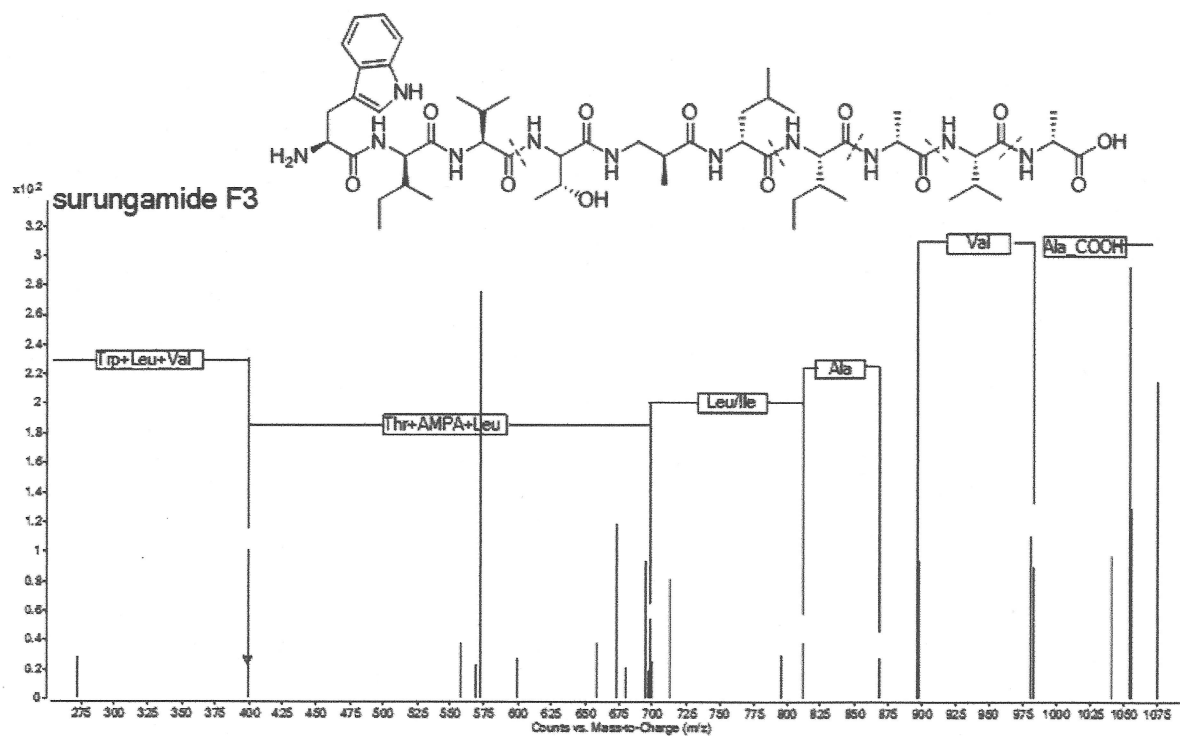


Figure S21. Biosynthetic model for surugamides in *S. albus* based on Ninomiya et al.¹⁰ SurA and SurD synthesize cyclic octapeptides (surugamides, acyl-surugamide, albucylones), while SurB and SurC are responsible for synthesizing linear decapeptides (surugamides F, F2, and F3).

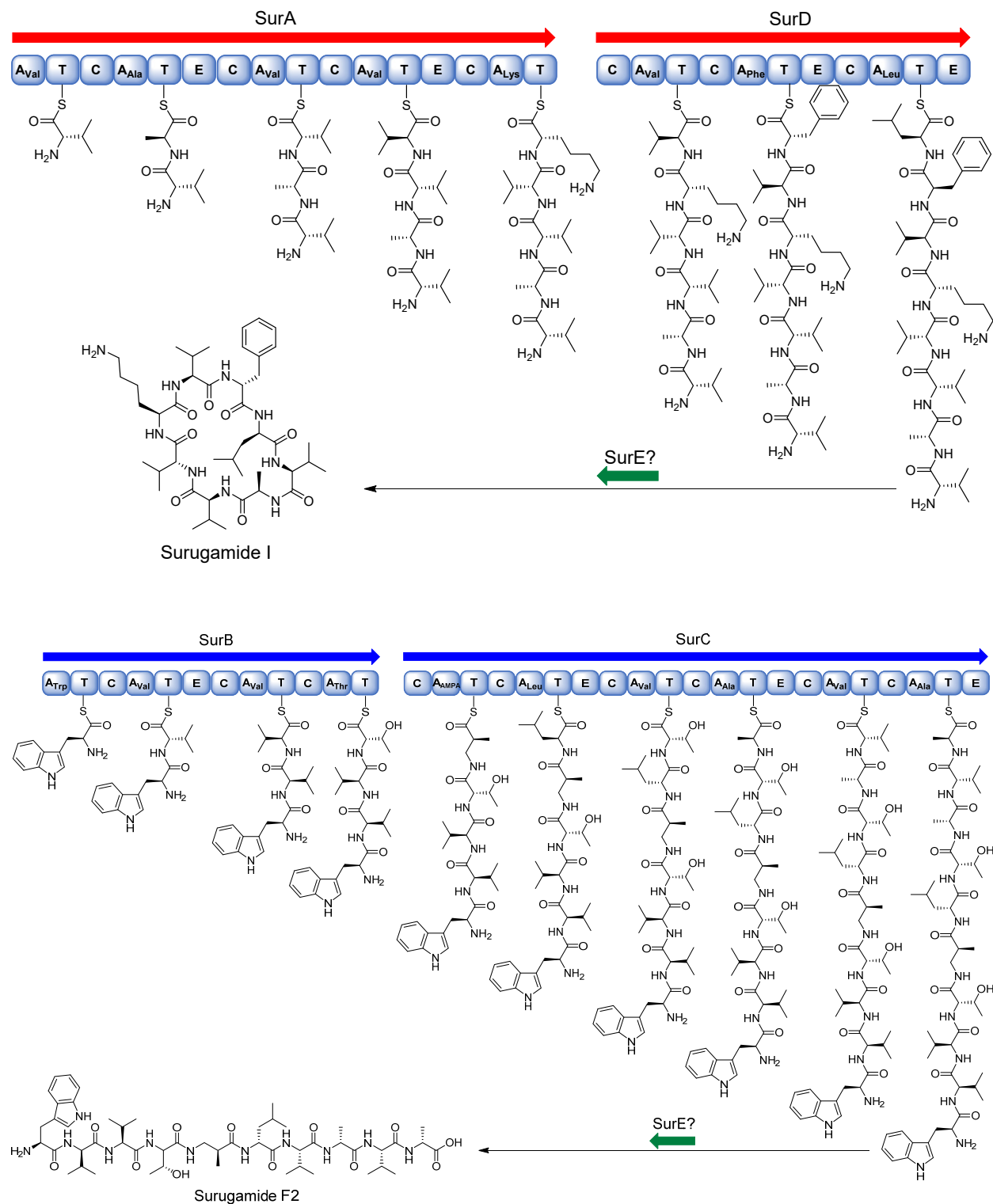
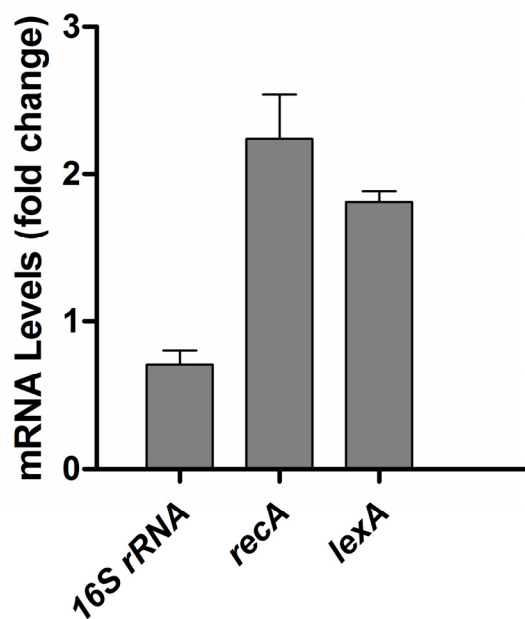


Figure S22. Induction of SOS response genes *recA* and *lexA* by etoposide. RT-qPCR was used to measure the transcriptional response of the SOS response genes *recA* and *lexA* to etoposide, which has been shown to inhibit DNA gyrase from actinobacteria.



Supplementary References

1. Bierman, M.; Logan, R.; O'Brien, K.; Seno, E.T.; Rao, R.N.; Schoner, B.E. *Gene* **1992**, *116*, 43-49.
2. Gust, B.; Kieser, T.; Chater, K. PCR targeting system in *Streptomyces coelicolor* A3(2). UK: The John Innes Foundation. (2002).
3. Kieser, T.; Bibb, M.J.; Buttner, M.J.; Chater, K.F.; Hopwood, D.A. Practical streptomyces genetics. The John Innes Foundation, Norwich, UK (2000).
4. Hosaka, T.; Ohnishi-Kameyama, M.; Muramatsu, H.; Murakami, K.; Tsurumi, Y.; Kodani, S.; Yoshida, M.; Fujie, A.; Ochi, K. *Nat. Biotechnol.* **2009**, *27*, 462-464.
5. Seyedsayamdost, M.R. *Proc. Natl. Acad. Sci. USA* **2014**, *111*, 7266-7271.
6. Shaner, N.; Stainbach, P.A.; Tsien, R.Y. *Nat. Methods* **2005**, *2*, 905-909.
7. Xu, F.; Kong, D.; He, X.; Zhang, Z.; Han, M.; Xie, X.; Wang, P.; Cheng, H.; Tao, M.; Zhang, L.; Deng, Z.; Lin, S. *J. Am. Chem. Soc.* **2013**, *135*, 1739-1748.
8. Hisawa, T.; Fujita-Yoshigaki, J.; Shirouzu, M.; Koide, H.; Sawada, T.; Sakiyama, S.; Yokoyama, S. *Cancer Lett.* **1993**, *69*, 161-165.
9. Takada, K.; Ninomiya, A.; Naruse, M.; Sun, Y.; Miyazaki, M.; Nogi, Y.; Okada, S.; Matsunaga, S. *J. Org. Chem.* **2013**, *78*, 6746-50.
10. Ninomiya, A.; Katsuyama, Y.; Kuranaga, T.; Miyazaki, M.; Nogi, Y.; Okada, S.; Wakimoto, T.; Ohnishi, Y.; Matsunaga, S.; Takada, K. *Chembiochem* **2016**, *17*, 1709-1712.